



OPEN ACCESS

EDITED BY

Liming Dai,
University of New South Wales, Australia

REVIEWED BY

Dipayan Pal,
University of California, San Diego,
United States
Gerardo Salinas,
Université de Bordeaux, France

*CORRESPONDENCE

Ichiro Imae,
✉ imae@hiroshima-u.ac.jp

RECEIVED 24 January 2024

ACCEPTED 24 February 2025

PUBLISHED 19 March 2025

CITATION

Imae I (2025) Potential-step
chronocoulometry for robust analysis of
charge-transport and thermoelectric
behaviors of conducting polymers.
Front. Mater. 12:1375558.
doi: 10.3389/fmats.2025.1375558

COPYRIGHT

© 2025 Imae. This is an open-access article
distributed under the terms of the [Creative
Commons Attribution License \(CC BY\)](https://creativecommons.org/licenses/by/4.0/). The
use, distribution or reproduction in other
forums is permitted, provided the original
author(s) and the copyright owner(s) are
credited and that the original publication in
this journal is cited, in accordance with
accepted academic practice. No use,
distribution or reproduction is permitted
which does not comply with these terms.

Potential-step chronocoulometry for robust analysis of charge-transport and thermoelectric behaviors of conducting polymers

Ichiro Imae*

Department of Applied Chemistry, Graduate School of Advanced Science and Engineering, Hiroshima University, Hiroshima, Japan

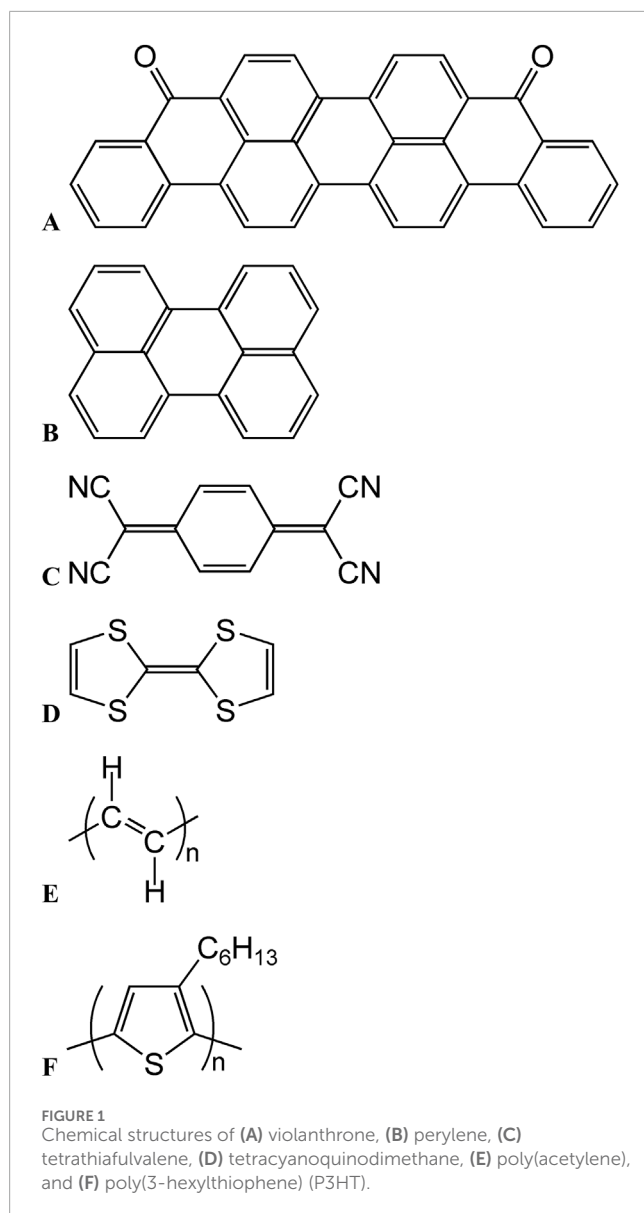
Since the groundbreaking discovery of polyacetylene films in the 1960s and subsequent efforts to enhance their electrical conductivity through halogen doping, several conductive π -conjugated polymers have been developed and applied in the fabrication of smart windows, organic photovoltaic cells, lithium-ion batteries, and other optoelectronic and electrical devices. Recently, the potential of these polymers for use in thermoelectric devices toward waste-heat recovery has drawn considerable attention. Given that the electrical properties of conducting polymers are strongly influenced by their doping state, the precise control of this state and accurate estimation of the doping level (charge density, i.e., the number of injected charges per unit volume) are of high importance. This review outlines the methods used to precisely control the doping state of conducting polymers and accurately determine their charge density, with a focus on potential-step chronocoulometry (PSC). Moreover, this paper highlights the recent progress in the application of PSC for analyzing charge-transport and thermoelectric properties. Challenges remain in the quantitative accuracy of electrochemical measurements, the applicability to a broader range of polymers, and the ability to distinguish between different charge carriers. Future research could resolve these issues and lead to improved understanding of charge transport and thermoelectric properties, paving the way for the development of advanced materials for thermoelectric applications.

KEYWORDS

conducting polymer, potential-step chronocoulometry, charge density, doping level, charge transport, thermoelectric property

1 Introduction

A fundamental characteristic of metallic compounds is their high conductivity, attributed to the presence of metallic bonds and free electrons. In contrast, organic compounds are mostly insulators and have traditionally been classified as such, thus finding numerous applications (e.g., dielectric materials, electrical insulation, building materials, and insulating films). A representative example is polyvinyl chloride, widely used to insulate metal wires in electrical cords. However, Akamatu and Inokuchi (1950) discovered that condensed polycyclic aromatic compounds, such as violanthrone (Figure 1A) and perylene (Figure 1B), can exhibit electrical conductivities of $\sim 10^{-10}$ S cm⁻¹ when doped with



halogens (e.g., bromine) despite their organic nature. Although this value is considerably lower than that of metals ($1\text{--}6 \times 10^5 \text{ S cm}^{-1}$) (Kittel, 2018), it is remarkably high for organic compounds, considering that insulating organic polymers exhibit conductivities on the order of $10^{-15} \text{ S cm}^{-1}$. Ferraris et al. (1973) reported that charge-transfer complexes formed by tetracyanoquinodimethane (Figure 1C) and tetrathiafulvalene (Figure 1D) exhibit metallic conductivity, which increases with decreasing temperature and reaches $3 \times 10^3 \text{ S cm}^{-1}$ at 40 K. These findings have drawn attention to the electrical properties of organic conducting compounds, especially those with conjugated π -electron systems.

However, the abovementioned materials are typically obtained as powders, which complicates their handling and the related fundamental investigations and applications. In contrast, polymeric compounds (e.g., polyethylene and polypropylene) can be converted to thin films and are therefore highly attractive from an industrial standpoint. Thus, the development of conductive polymers has

drawn considerable interest. Previous research suggests that conductive organic compounds must have structures with well-developed conjugated π -electron systems similar to those of aromatic compounds. Theoretical predictions pioneered by Bayliss (1948) support this expectation, suggesting that a hypothetical infinitely long polyene loses bond alternation and becomes metallic. However, with increasing molecular length, polyenes become less soluble in organic solvents, and their separation and isolation after synthesis become difficult. Natta et al. (1967) used catalytic acetylene polymerization to synthesize polyacetylene (Figure 1E) with chain lengths approaching infinity, isolating this material as a black, insoluble, and infusible powder. Subsequent studies actively focused on polyacetylene synthesis; in the 1960s, Shirakawa realized the well-reproducible synthesis of polyacetylene films by optimizing catalyst concentration (Ito et al., 1974; Shirakawa and Ikeda, 1971; Shirakawa et al., 1973). Later, Shirakawa et al. (1977) achieved a high electrical conductivity of $1 \times 10^2 \text{ S cm}^{-1}$ by doping polyacetylene thin films with halogens, such as bromine and iodine. The ability of conductive organic compounds to be obtained as films was recognized to be crucial for property evaluation and device fabrication. The success of thin-film formation became pivotal for the development of conducting polymers (Heinze et al., 2010; Swager, 2017), ultimately earning Shirakawa, MacDiarmid, and Heeger the (Nobel Prize in Chemistry, 2000).

In the abovementioned research of Akamatu and Inokuchi (1950) and Shirakawa et al. (1977), doping processes were noted to be crucial for π -conjugated compounds such as perylene and polyacetylene to demonstrate electrical conductivity. Doping involves the extraction (oxidation reactions) or injection (reduction reactions) of electrons from or into π -conjugated compounds, respectively. Alternatively, oxidation reactions can be viewed as the injection of positive charges (holes). During redox reactions, counterions (anions for oxidation and cations for reduction) are introduced to maintain the overall electrical neutrality of the system. From the perspective of π -conjugated compounds, this introduction of “impurities” (counterions) is referred to as “doping,” and the counterions introduced to maintain electrical neutrality are termed “dopant” ions.

Doping is typically achieved through two strategies. Chemical doping, used by researchers such as Akamatu and Inokuchi (1950) and Shirakawa et al. (1977), involves the addition of oxidants (such as halogens or iron chloride) or reductants (such as lithium or sodium metal) to π -conjugated compounds to inject charges via electron-transfer reactions. Notable examples are the reactions of perylene or polyacetylene with halogens, in which positive charges are injected. This method has been widely used because of its simplicity. However, the reaction between π -conjugated compounds and redox agents is affected by their redox potentials, which complicates doping-state control. Additionally, the accurate quantitation of the charge density (i.e., the number of charges injected into π -conjugated compounds per unit volume) is challenging for numerous systems. In particular, π -conjugated compounds are typically doped with excess oxidants or reductants, and the doping state of these compounds depends on the oxidant/reductant capacity, which makes the quantitation of the charge-transfer extent impossible. The second strategy, namely electrochemical doping, exploits electrode reactions and enables the precise control of the doping state of π -conjugated

compounds through the adjustment of the electrode potential. Furthermore, by measuring the amount of charge flowing during the electrode reaction using a coulometer, one can accurately determine the charge density. Our research group has successfully controlled and quantified the charge density of π -conjugated oligomers and polymers using potential-step chronocoulometry (PSC), leveraging the characteristics of electrochemical doping. We found that utilizing this PSC technique for the precise control and accurate quantification of carrier density in π -conjugated polymers is effective and crucial, not only from the perspective of fundamental research on the charge-transport mechanism in conducting polymers, as discussed in Section 3, but also from the viewpoint of practical research as a valuable tool for establishing design guidelines to enhance the performance of organic thermoelectric materials, which have recently garnered attention as new energy materials in industry, government, and academia, as detailed in Section 4.

In this review, we explain the principles of PSC, outline a PSC-based method for the simultaneous measurement of charge density and electrical conductivity, and summarize the findings of our research on the charge-transport and thermoelectric properties of oligo- and polythiophenes with well-defined structures.

Additionally, doping techniques include “secondary doping,” which enhances existing conductivity and stability through the addition of high-boiling-point solvents such as ethylene glycol and dimethyl sulfoxide (Hohnholz et al., 2005; Ashizawa et al., 2005; Okuzaki et al., 2009; Murakami et al., 2011), as well as non-volatile ionic liquids like imidazolium salts (Döbbelin et al., 2007; Badre et al., 2012; Liu et al., 2012; Kee et al., 2016; Mazaheripour et al., 2018; Saxena et al., 2019; Li et al., 2022; Imae et al., 2022). However, since this topic lies outside the scope of this review, we will focus on primary doping techniques aimed at charge injection and quantification.

2 PSC method

Potential-Step Chronocoulometry (PSC) is an electrochemical technique utilized to investigate charge transfer processes across a variety of materials. One of its key advantages is the ability to quantitatively estimate the apparent charge-carrier densities in π -conjugated polymers. By applying a sudden change in voltage (or potential) to an electrode within an electrochemical cell, researchers can measure the transient current response over time, providing valuable insights into the electric charges that are either extracted from or introduced into the compounds through oxidation and reduction processes.

Another significant feature of the PSC technique is its capability to precisely control the redox state of compounds by adjusting the applied electrode potential. This allows for the estimation of the charge-carrier density of π -conjugated polymers at each specific electrode potential, enabling the analysis of their properties in various controlled charge states.

By employing the PSC method, we can systematically analyze the correlation between physical properties and carrier density. This is accomplished by quantifying the charge-carrier density of π -conjugated polymers at each controlled charge state and evaluating the associated physical properties of the polymers.

In our research group, we have leveraged this systematic approach to deepen our understanding of the relationship between carrier density and the charge-transport and thermoelectric properties of π -conjugated polymers. This investigation is vital for the development of advanced materials with enhanced performance across various applications, including thermoelectric devices.

From this point onward, we will detail the experimental procedures for applying the PSC method, using poly(3-hexylthiophene) (P3HT, Figure 1F) as a representative example of a π -conjugated polymer. PSC requires a deep understanding of sample electrochemical features, especially redox potentials. Therefore, before PSC, cyclic voltammetry tests were conducted using a three-electrode system with a sample-coated indium-doped tin oxide (ITO) or platinum plate as the working electrode, platinum wire as the counter electrode, and Ag/Ag⁺ as the reference electrode (Figure 2A). The organic electrolyte solution was prepared by dissolving organic salts (such as tetraethylammonium perchlorate (Et₄NClO₄) or tetrabutylammonium tetrafluoroborate (Bu₄NBF₄)) in a solvent that does not dissolve the sample film (e.g., acetonitrile). The cyclic voltammogram of P3HT (Figure 2B) showed no current at -0.4 V vs. Ag/Ag⁺, which indicated that P3HT was in a neutral state. As the electrode potential transitioned to the positive side from -0.4 V, an anodic current was observed at ~0.2 V vs. Ag/Ag⁺ when electrons were withdrawn from P3HT through the working electrode into the external circuit, suggesting the oxidation of P3HT (p-type doping) at this potential. In contrast, when the electrode potential was reversed to the negative side from 0.8 V vs. Ag/Ag⁺, a cathodic current was observed (the electrons were transferred from the electrode to the oxidized P3HT). This outcome indicated that at this potential, the oxidized (p-type doped) P3HT received electrons (i.e., was reduced) and returned to the neutral state. Finally, when the electrode potential returned to ~0 V vs. Ag/Ag⁺, no current flowed in the system, which suggested that P3HT had returned to the neutral state.

The insights obtained from cyclic voltammetry results were applied to perform PSC measurements on P3HT (Figure 3A). The initial potential (E_0) was set as -0.4 V vs. Ag/Ag⁺, at which no redox reaction occurred. Subsequently, the P3HT film was oxidized at a certain potential (E_1) by stepping the electrode potential from -0.4 V vs. Ag/Ag⁺. The time-dependent current associated with the oxidation (doping) reaction during this potential step (-0.4 \rightarrow E_1) was integrated using a coulometer to monitor the electric charge (Q_1^{dope}) required for the oxidation of P3HT at E_1 . After the estimation of the electric charge at E_1 , the electrode potential was returned to initial potential E_0 to reduce (dedope) the oxidized (doped) P3HT back to the neutral state, and the electric charge (Q_1^{dedope}) associated with this reduction current was measured. In general, for a reversible redox reaction, Q_1^{dope} must equal Q_1^{dedope} . Dividing this electric charge ($Q_1^{\text{dope}} = Q_1^{\text{dedope}} \equiv Q_1$) by the elementary charge (e) yields the number of positive charges introduced into the P3HT film. Furthermore, by calculating the volume (V) of the employed P3HT film and using it to normalize the number of charges, one can determine the charge density (n_1) introduced into P3HT at the potential E_1 (with $x = 1$ in Equation 1). Similarly, in the $E_0 \rightarrow E_2 \rightarrow E_0$ oxidation-reduction process, we can measure the charge density (n_2) at the potential E_2 , and in the $E_0 \rightarrow E_x \rightarrow E_0$ process, we can measure the charge density at the potential E_x . Finally, the charge density n_x can be accurately evaluated as a

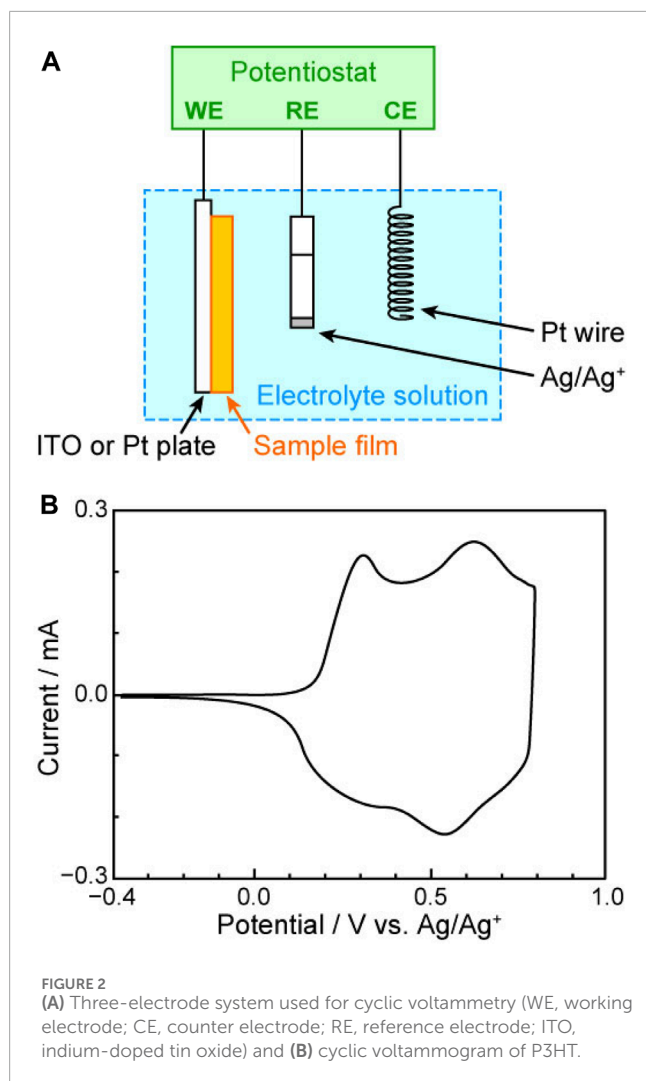


FIGURE 2
(A) Three-electrode system used for cyclic voltammetry (WE, working electrode; CE, counter electrode; RE, reference electrode; ITO, indium-doped tin oxide) and (B) cyclic voltammogram of P3HT.

function of the potential E_x (Figure 3B). Moreover, the stabilization time at each potential step in PSC measurements is essential to ensure that the oxidation and reduction reactions are complete. The current is allowed to decrease and stabilize to a low level, ensuring that influences such as contact resistance and ion transfer rates are minimized. To confirm that each oxidation and reduction process is Faradaic, we carefully selected adequate stabilization times to maintain the accuracy and reliability of the measurements. The stabilization time was approximately 5 min, allowing the change in the amount of coulombs measured by the coulometer to reach saturation.

$$n_x = \frac{(Q_x/e)}{V} \quad (1)$$

In the case of oligomers or polymer films with clear repeating units, such as P3HT, the doping level is typically used as an indicator of the doping state instead of charge density and can be calculated as follows (In cases like PEDOT:PSS, where the polymer is inherently doped with counterions (e.g., PSS), the term “oxidation level” is often more appropriate, as dedoping does not result in counterion removal. For simplicity, we refer to this as the “doping level” throughout the manuscript.). The electric charge (Q) monitored

in the redox reaction by the coulometer is divided by the Faraday constant (F) ($= Q/F$) to obtain the amount (moles) of charge introduced into the target polymer film. Next, the weight of the polymer film, calculated from the film volume (V) and density (d) ($= V \times d$), is divided by the molecular weight of the monomer units of the macromolecule (M) constituting this film ($= (V \times d)/M$) to obtain the amount (moles) of these units. Finally, the doping level is calculated according to Equation 2 and used to examine the amount of charge injected per monomer unit, thus facilitating the correlation of carrier species such as (bi)polarens:

$$\text{doping level (\%)} = \frac{Q/F}{(V \times d)/M} \times 100 \quad (2)$$

While other complementary techniques, such as Hall effect measurement, X-ray photoelectron spectroscopy (XPS), organic electrochemical transistor (OECT), and electrochemical quartz crystal microgravimetry (EQCM) measurements, are available for estimating doping or oxidation levels, each method has limitations. Hall effect measurements, for instance, require relatively high electrical conductivity in the sample to obtain accurate results, which may not be feasible for all polymers. XPS can determine doping levels by analyzing the signal area ratios of elements unique to the polymer or dopant ions; however, as a surface-sensitive method, XPS does not accurately reflect the doping level throughout the entire sample. OECT measurements operate in a similar system to our approach (Salinas and Frontana-Urbe, 2019; Nicolini et al., 2024), but they do not allow for precise control of the polymer’s charge state or quantitative evaluation of carrier density, as is possible with the PSC method. Although the EQCM method is a powerful tool for analyzing the electrochemical redox reactions of conductive polymers (Bose et al., 1992), it is very quantitative in the sense that it can determine the weight of ions entering and exiting the conductive polymer film during redox reactions. However, this method cannot directly quantify the extent of charge transfer that occurs, and thus, it is not a technique that can directly quantify the amount of charge transfer.

3 Simultaneous measurement of electrical conductivity and doping level

Our research group has developed a PSC-based method for the simultaneous measurement of electrical conductivity and charge density at various doping states, commonly known as *in situ* conductivity measurement. The corresponding measurement system is a modification of a conductivity measurement system established previously (Fäid and Leclerc, 1994; Lankinen et al., 1998; Morvant and Reynolds, 1998; Schiavon et al., 1989; Thackeray et al., 1985; Zotti, 1998), incorporating a coulometer for the concurrent measurement of electrical conductivity and charge density (Harima et al., 1998; 1999; 2000; Imae et al., 2015a; Kunugi et al., 2000; Tang et al., 2000). Unlike the three-electrode system used in the previously discussed PSC-based method, this system comprises four electrodes (A–D) and two potentiostats (1 and 2) (Figure 4A). Among these four electrodes, three are connected to potentiostat 1, serving as the working electrode (A), counter electrode (B), and reference electrode (C) for PSC

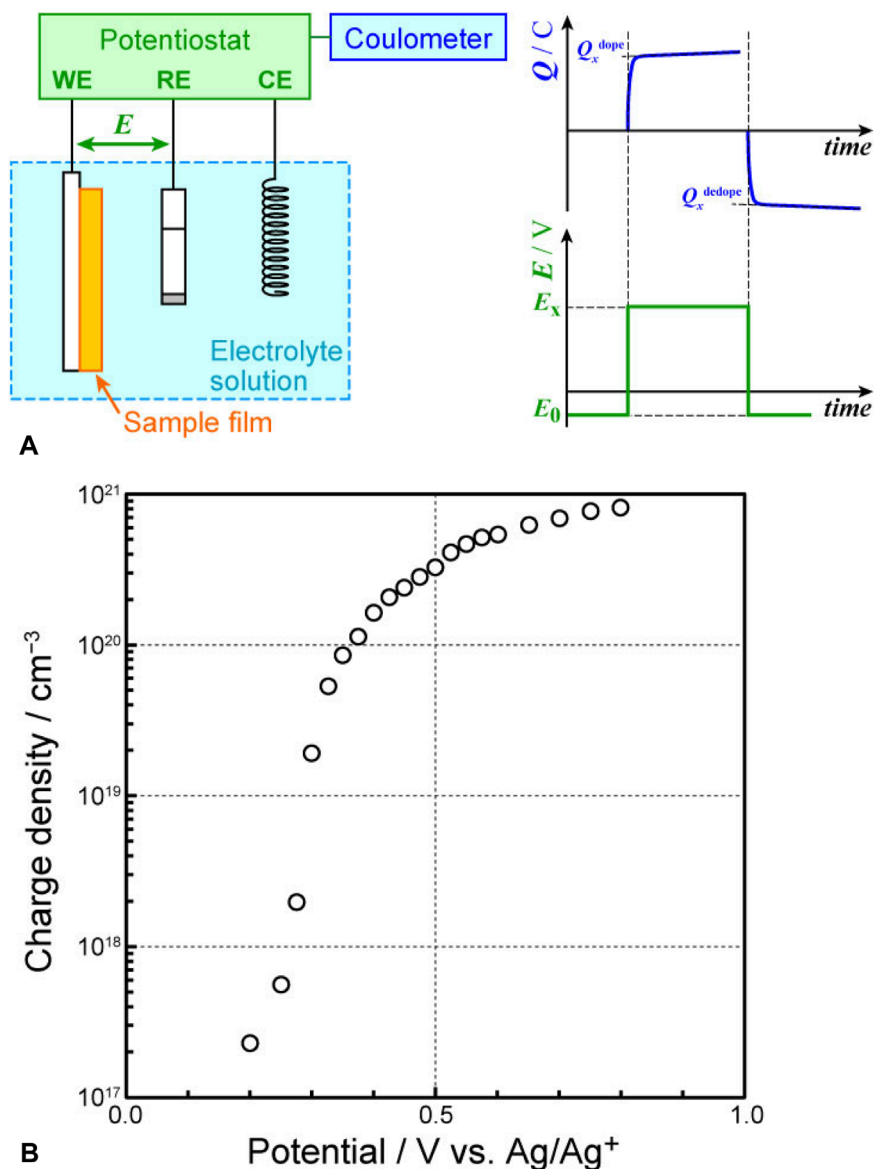


FIGURE 3 (A) Setup used for potential-step chronocoulometry (PSC) and (B) correlation between applied electrode potential and charge density.

conducted using a coulometer to measure charge density (or doping level). A certain potential (E_{A-C}) is applied between electrodes A and C during PSC with potentiostat 1, whereas a small triangular wave potential difference of ± 1 mV (E_{A-D}) is applied between electrodes A and D using potentiostat 2. As electrode A is connected to the working electrodes of both potentiostats and the potential difference between electrodes A and D is negligible (within ± 1 mV) in relation to that between electrodes A and C, the potentials of electrodes A and D are similar. Consequently, the doping state of the sample between electrodes A and D is nearly uniform. By measuring the current flowing between electrodes A and D in this state using potentiostat 2, one obtains the current–voltage characteristics shown in Figure 4B. The reciprocal of the slope of this line can be used to determine the resistance (R) of the sample between electrodes A and D. Additionally, by calculating the cross-sectional

area (A) of the sample using its thickness (t) and electrode width (w), and considering the distance (L) between electrodes A and D, one can determine the electrical resistivity (ρ) of the sample using Equation 3. Notably, if the sheet resistance (R_s) can be measured, the electrical resistivity can be estimated as $\rho = R_s \times t$. Finally, the electrical conductivity (σ) can be calculated as the reciprocal of ρ ($\sigma = \frac{1}{\rho}$). In this manner, correlations between the electrode potential and electrical conductivity can be established (Figure 4C). In this measurement, electrical resistance was determined using a two-electrode system as follows. For the electrodes, a two-band probe with an interelectrode distance of approximately 100 μm was used in the high doping region, while a comb-shaped electrode (ALS Co., Ltd., 65 lines, 5 μm interelectrode distance, total electrode width of 260 mm) was employed in the low doping region to counteract the increase in resistance. A polymer thin film was deposited onto these

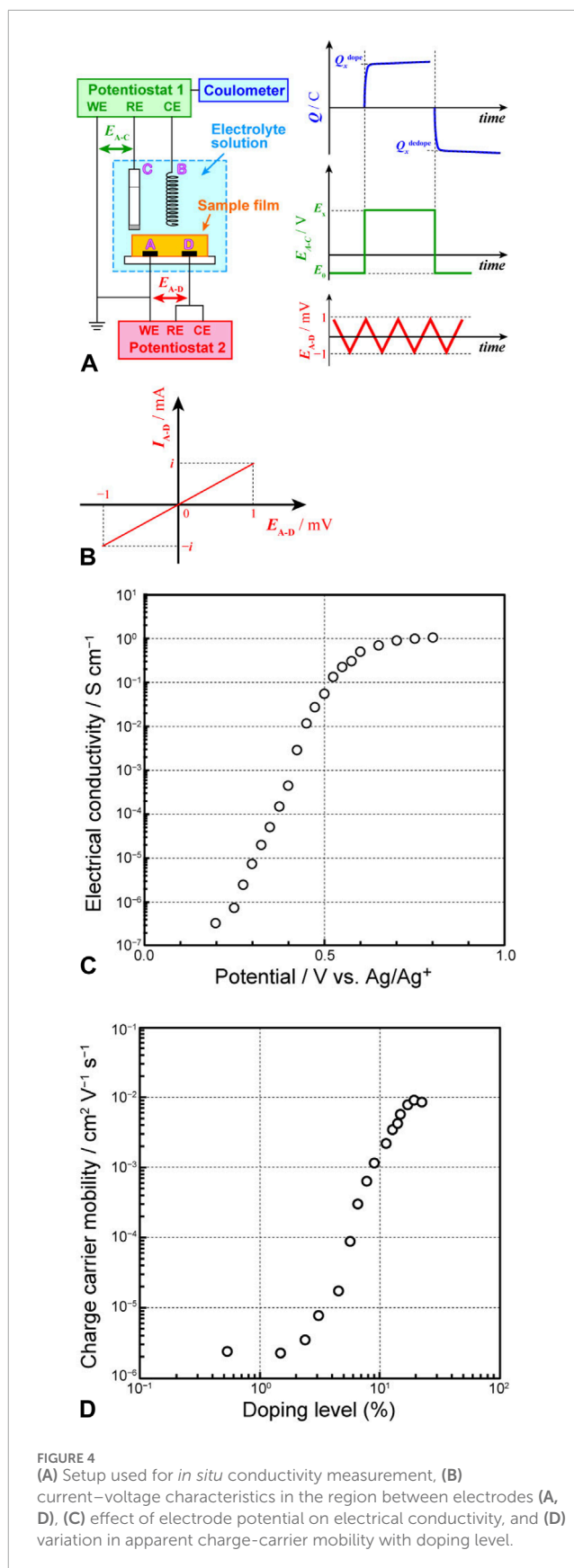
electrodes by spin coating. The thickness of the resulting polymer film was measured using a Keyence VK-9700 3D laser microscope and was found to be around 50 nm. Furthermore, considering the relationships among the electrical conductivity, charge density (n), elementary charge (e), and charge mobility (μ) (Equation 4), one can calculate the apparent charge mobility at each doping level from the estimated charge density and electrical conductivity obtained using this system (Figure 4D):

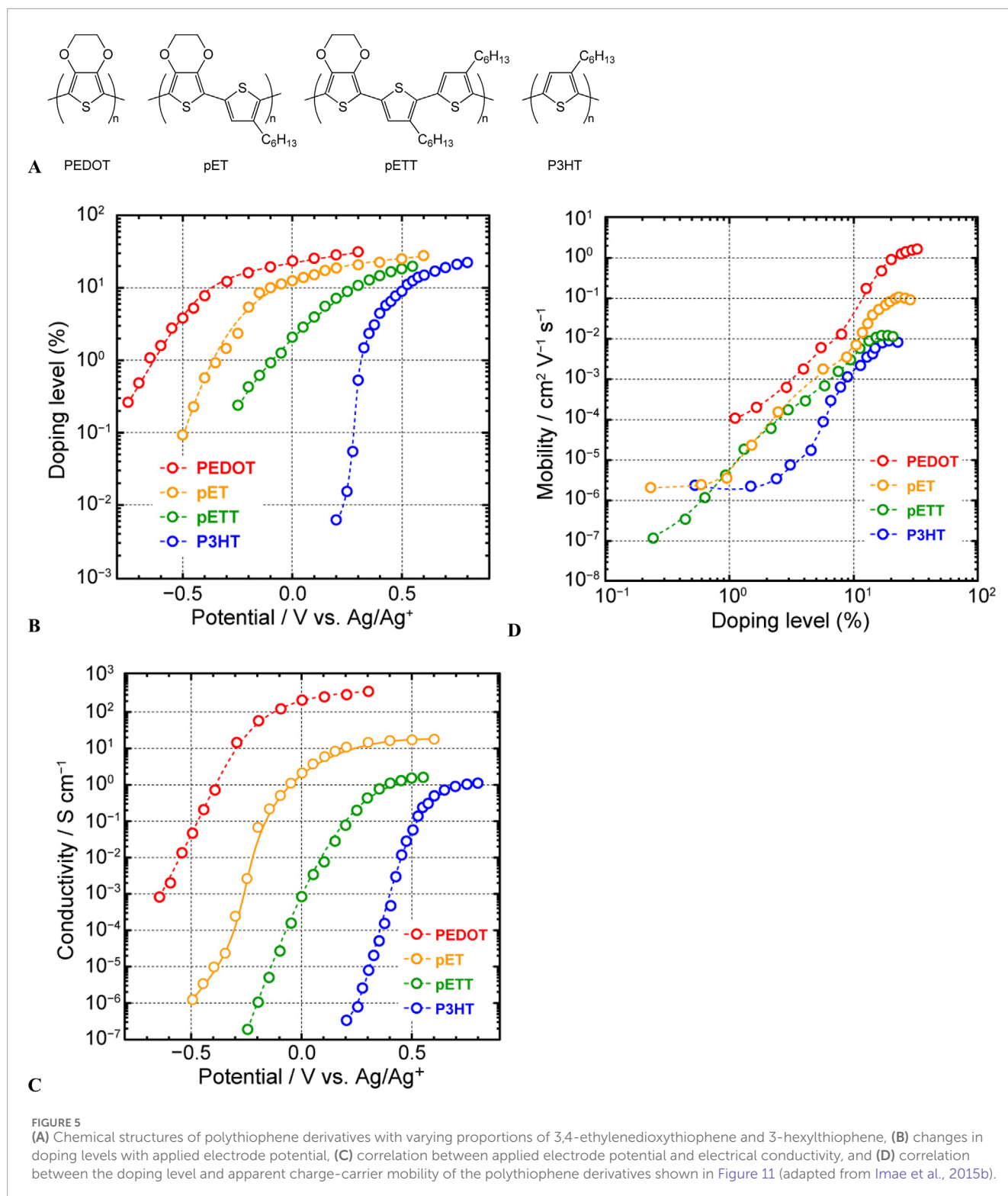
$$R = \rho \frac{L}{A} = \rho \frac{L}{t \times w} = \frac{\rho}{t} \times \frac{L}{w} = R_s \times \frac{L}{w} \quad (3)$$

$$\sigma = n \times e \times \mu \quad (4)$$

Below, an illustrative application of this measurement system is discussed. Our group previously synthesized several polythiophenes with varying contents of 3,4-ethylenedioxythiophene (EDOT) through its copolymerization with 3-hexylthiophene (Figure 5A) (Imae et al., 2015b). However, we had difficulty conducting meaningful comparisons of polymers with different doping states to examine the charge-transport properties of these compounds as functions of molecular structure. However, the use of this system enabled a systematic discussion. Each polymer showed an increase in the doping level with increasing applied voltage, ultimately reaching saturation (Figure 5B). The saturation doping level increased with the proportion of EDOT units in polythiophene. This outcome suggested that higher doping levels can be achieved in polythiophenes with higher proportions of the electron-donating EDOT units, as these units can stabilize the positive charges introduced into the polymer. For each polymer, the electrical conductivity increased with the applied voltage, reaching saturation at a certain point (Figure 5C). This trend, similar to the change in the doping level (a linear increase followed by saturation), suggested that the increase in electrical conductivity is associated with an increase in charge density. However, the change in the electrical conductivity spanned 5–6 orders of magnitude, whereas the doping level varied only by 2–3 orders of magnitude. Therefore, we analyzed the charge mobility estimated from the doping level and electrical conductivity and observed that the charge mobility varied by 4–5 orders of magnitude with the change in the doping level (Figure 5D). This variation was attributable to the transformation of the charge carriers from polarons, characterized mainly by hopping conduction and low mobility, to bipolarons, exhibiting metallic conduction and high mobility, with doping level variation. The spectroelectrochemical properties of the polymer film also highlighted the changing behavior of charge carriers.

As another illustration, we applied our method to the investigation of the charge-transport properties of oligothiophenes with well-defined structures. Oligothiophenes, originally considered model compounds for polythiophenes, have been extensively investigated in terms of the correlations between the molecular structure and optical, electrochemical, and electrical properties, including conjugated-chain length. Moreover, the discovery of their exceptional optical and electrical properties, originating from the controlled structures, has highlighted the potential of oligothiophenes as a new group of photo- and electroactive





materials. Since then, oligothiophenes have been used in various applications, such as electrochromic display devices (Imae et al., 1995; 1997a; Nawa et al., 1993a; Ohseido et al., 1996) and field-effect transistors (Garnier et al., 1996; Hajlaoui et al., 1997; Hajlaoui et al., 2004; Hajlaoui et al., 2002; Horowitz et al., 1996). We developed novel polysilsesquioxanes containing thiophene oligomers with

8–12 units (PBSO n T, $n = 8, 10, 12$, Figure 6A) and investigated their charge-transport properties (Imae et al., 2009; Imae et al., 2011; Imae et al., 2012b). Owing to the unique characteristics of the siloxane network of polysilsesquioxanes, the polymer films could firmly adhere to the surfaces of glass or metal-oxide substrates. Moreover, the doped oligothiophene sites imparted

electrical conductivity and visible-light transparency. Owing to these characteristics, PBSO n T could be used to fabricate transparent conductive films with high mechanical strength (Imae et al., 2012a; Imae et al., 2017b; Tsukada et al., 2020). For all polymers, the doping level increased with increasing applied voltage, ultimately reaching ~20% (Figure 6B), equivalent to all oligothiophene moieties in the film being two-electron-oxidized. Furthermore, with the increase in the applied voltage and doping level, the electrical conductivity increased from 10^{-6} S cm $^{-1}$ in the neutral state to the maxima of 5×10^{-3} S cm $^{-1}$ (PBSO8T), 1×10^{-2} S cm $^{-1}$ (PBSO10T), and 3×10^{-2} S cm $^{-1}$ (PBSO12T) after doping (Figure 6C). The maximum electrical conductivity increased with the increasing molecular-chain length of the introduced oligothiophene units. To gain detailed insights into the charge-transport properties of these polymer films, we established charge mobility–doping level correlations (Figure 6D). At low doping levels (<1%), the mobility of all films was $1\text{--}2 \times 10^{-6}$ cm 2 V $^{-1}$ s $^{-1}$, and charge transport in this range could be explained by the interchain hopping conduction of one-electron-oxidized species. The mobility increased with increasing doping level, peaking at levels of 10%–15%, which corresponded to a state with coexisting one- and two-electron-oxidized oligothiophenes. In the regions with doping levels of >20%, as mentioned above, nearly all oligothiophenes in the film were in a two-electron-oxidized state, hindering the movement of positive charges (holes) owing to the considerable Coulomb repulsion. Therefore, in PBSO8T, which featured a short oligothiophene chain length, the effect of this Coulomb repulsion was substantial, markedly reducing mobility. In contrast, in PBSO10T and PBSO12T, which had longer oligothiophene chains, the effect was alleviated, and the decrease in mobility intensified. Additionally, we investigated the charge-transport properties of oligothiophenes without any polymer chains (undecathiophene and dodecathiophene) (Imae et al., 2013; Imae et al., 2020b). These oligothiophenes, with molecular weights comparable with those of polythiophenes, formed homogeneous films upon spin-coating without being linked to unconjugated polymer chains, such as polyethylene (Imae et al., 1997b; Nawa et al., 1993b; Nawa et al., 1995), polymethacrylate (Ohsedo et al., 1999; Ohsedo et al., 2000; Ohsedo et al., 2003), or polysilsesquioxane (Imae et al., 2009; Imae et al., 2011; Imae et al., 2012b). Moreover, the electrical conductivity of these oligothiophenes increased upon electrochemical doping, reaching a maximum of 0.7–1.0 S cm $^{-1}$.

4 Application to thermoelectric-parameter analysis

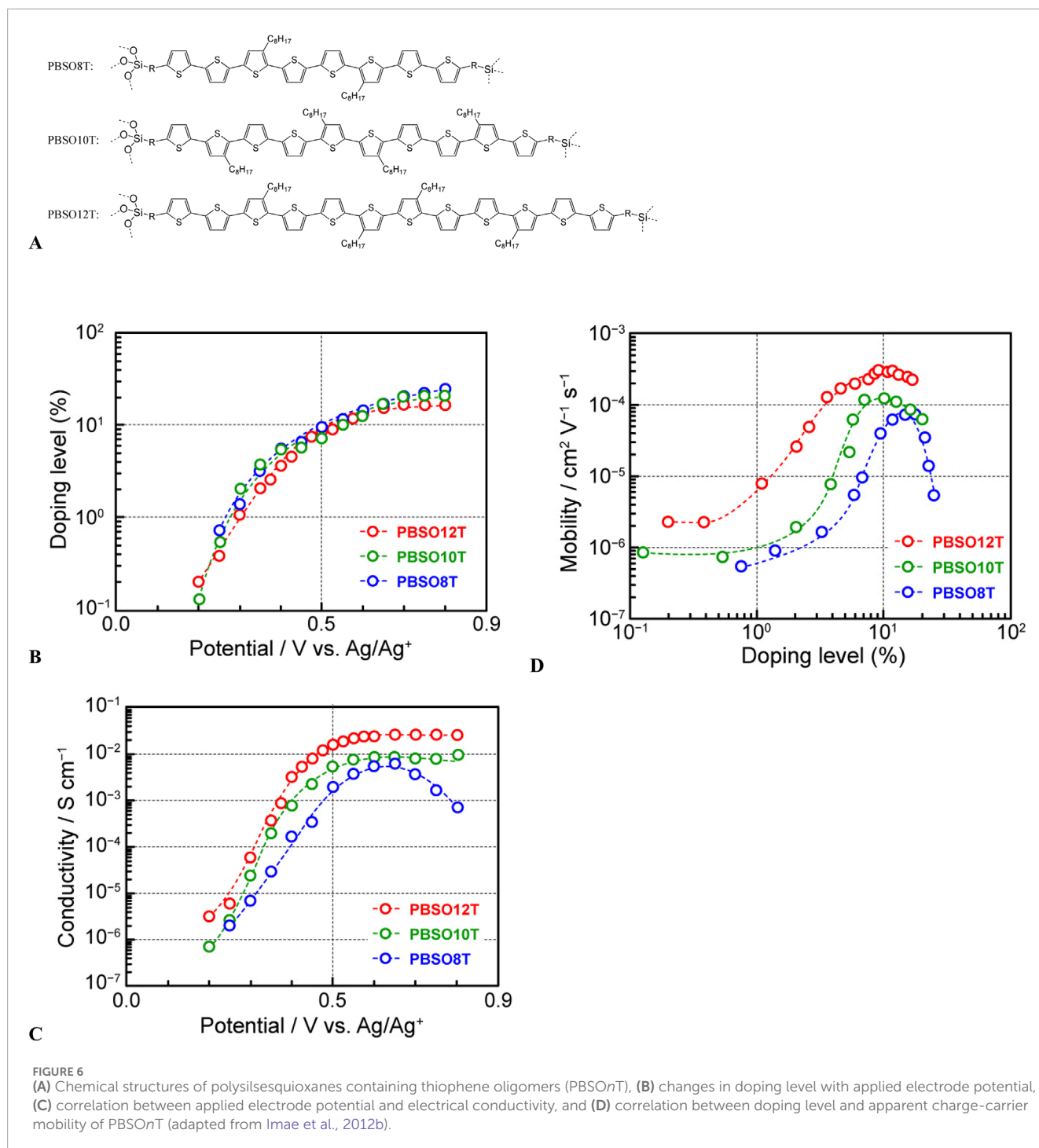
A large amount of thermal energy originating from power plants, automobiles, factories, and other sources is often discarded without appropriate utilization (Francioso and De Pascali, 2017; Kishore et al., 2019; Lee, 2017). Table 1 summarizes the field-specific waste-heat data for Japan in 2000, indicating an annual emission of ~2 million Tcal of thermal energy (Sugimoto, 2000), equivalent to that from 270 nuclear reactors with capacities of ~1 GW (total annual power generation of ~7,500 Tcal/year). Although some of this waste heat is used for power system maintenance, hot water supply, and heating, a considerable amount is discarded. Thus, the development of thermoelectric devices capable of recovering this unused thermal energy as electrical energy has attracted

the considerable attention of academia, industry, and government (Boston et al., 2017; Coughlan et al., 2017; Gayner and Kar, 2016; Koumoto and Mori, 2013; Ravichandran, 2017; Tan et al., 2016; Yin et al., 2017; Zhu et al., 2017). The use of inorganic compounds in thermoelectric devices has already been practicalized, with these devices currently serving as power sources for space probes (such as Voyager and Cassini) and domestic devices (such as small electric refrigerators). However, ~70% of waste heat is generated at mid- to low-temperatures of <200°C, at which most inorganic thermoelectric materials cannot operate efficiently (Figure 7). The inorganic thermoelectric materials efficiently operating in this temperature range are limited to bismuth telluride (Bi $_2$ Te $_3$) and its derivatives, which unfortunately contain rare (Bi) and highly toxic (Te) elements. Therefore, from the perspective of waste-heat utilization, the practical use of inorganic thermoelectric materials is limited.

Professor Toshima (Yan and Toshima, 1999) demonstrated the potential of conducting polymers as thermoelectric materials. Compared with their inorganic counterparts, organic thermoelectric materials are characterized by cost-effectiveness, low weight, low toxicity, flexibility, and printability; therefore, they serve as suitable power sources for wearable electronic devices and sensors used in the Internet-of-Things applications. Recently, researchers worldwide have focused on organic thermoelectric materials. In 2016, Professor Toshima and Professor Kawai launched the International Conference on Organic and Hybrid Thermoelectrics, which focused on organic materials (Toshima and Kawai, 2017). Since then, the research and development of organic thermoelectric materials has experienced exponential growth (Figure 8) (Katz and Poehler, 2016; Kroon et al., 2016; Lei et al., 2017; Li and Lei, 2021; Masoumi et al., 2022; Peng et al., 2017; Russ et al., 2016; Toshima, 2017; Yao et al., 2018; Zhao et al., 2020). The materials studied as organic thermoelectrics can be broadly categorized into conducting polymers and carbon nanotubes. The performance of thermoelectric materials is typically evaluated by the dimensionless figure of merit (ZT) defined in Equation 5, with higher ZT values indicating better thermoelectric performance. ZT values exceeding unity ($ZT \geq 1$) are considered the benchmark for practical applications.

$$ZT = \frac{S^2 \sigma}{\kappa} T = \frac{PF}{\kappa} T \quad (5)$$

where S , σ , κ , T , and PF are the Seebeck coefficient, electrical conductivity, thermal conductivity, absolute temperature, and power factor ($PF = S^2 \sigma$), respectively. Among the organic thermoelectric materials, carbon nanotubes exhibit remarkably high electrical conductivities and Seebeck coefficients, thus featuring excellent power factors. However, the high thermal conductivity of these nanotubes (~ 1000 W m $^{-1}$ K $^{-1}$) results in low ZT . In contrast, conducting polymers, with a thermal conductivity of 0.2 W m $^{-1}$ K $^{-1}$ (almost four orders of magnitude lower than that of carbon nanotubes), exhibit improved ZT values but low electrical conductivities and Seebeck coefficients while featuring high power factors. Despite these limitations, conducting polymers offer additional advantages, such as the ability to customize molecular skeletons through organic synthetic chemistry, which enables control over their physical properties. Moreover, the thermoelectric properties of conducting polymers prepared by doping π -conjugated polymers can potentially be controlled by adjusting the doping



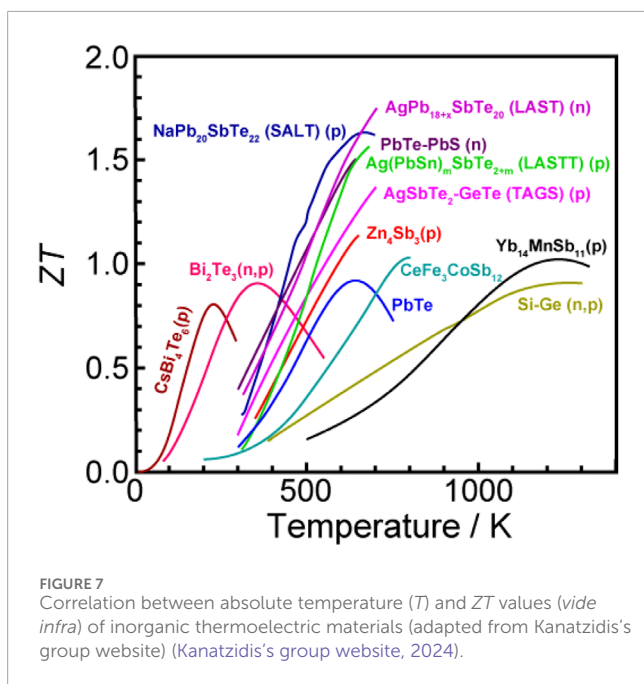
conditions (such as doping levels and the chemical structures of dopant ions). Therefore, we investigated the thermoelectric performance of conducting polymers by controlling and quantifying doping levels through PSC and attempted to clarify the effects of the chemical structure of π -conjugated polymers and dopant ions on the thermoelectric performance of such polymers.

The setup used for the *in situ* measurement of electrical conductivity cannot be directly used to investigate thermoelectric properties. Therefore, after controlling and quantifying doping levels through PSC, one should detach the conducting polymer film from

the working electrode and evaluate its electrical conductivity and Seebeck coefficient with reference to those of the freestanding film. In the cases when freestanding films were challenging to obtain because of their high brittleness or susceptibility to rupture, we fabricated polymer films on ITO and silica glasses of the same size under identical conditions. Chemical doping was then performed in the same solution, and the doping state was controlled by adjusting the immersion time of the polymer film in the doping solution. The doping level of the polymer film was estimated for the film coated on ITO through PSC. Subsequently, the

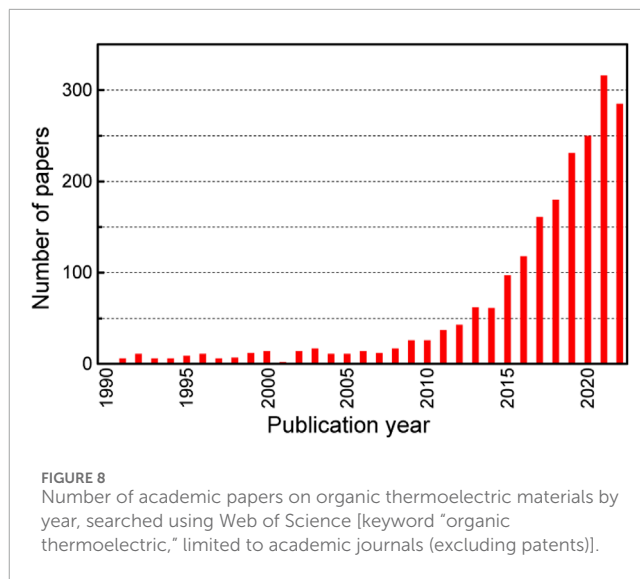
TABLE 1 Field-specific waste-heat data for Japan in 2000.

Exhaust heat discharge point	Amount of exhaust heat (Tcal/year)
Thermal power plants	858,631
Nuclear power plants	406,720
Automobiles	458,184
Factories	197,236
Incineration furnaces	75,200
Decentralized power generations	53,647
Renewable energies	20,193
Total	2,069,811



thermoelectric properties were measured for the film coated on silica glass (Figure 9).

Figure 10 shows the thermoelectric properties of P3HT with doping levels controlled and quantified through PSC (Imae et al., 2018). Similar to the results of *in situ* measurements, the electrical conductivity of P3HT in the freestanding film increased with increasing doping level and reached saturation, whereas the Seebeck coefficient decreased at higher doping levels. This trade-off is commonly observed in inorganic thermoelectric materials. When P3HT is electrochemically doped, anions in the electrolyte solution are introduced into the polymer film as dopant ions. Therefore, to investigate the effects of modifying the chemical structure of the supporting electrolyte used for electrochemical doping, we doped P3HT with two types of dopant ions, ClO_4^- and PF_6^- , revealing that this modification had a minimal impact on the electrical

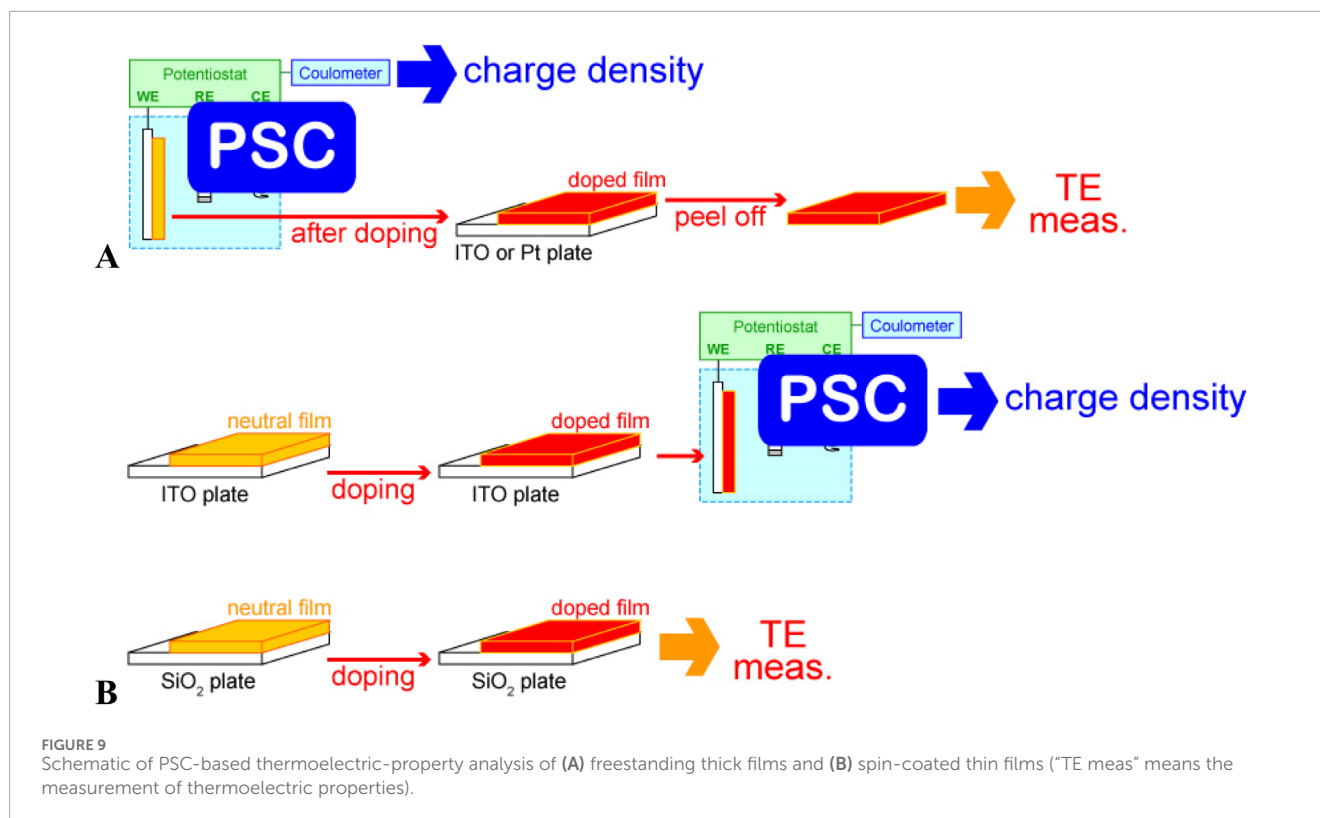


conductivity and Seebeck coefficient. Furthermore, to examine the effects of different doping methods, we chemically doped P3HT using nitrosonium hexafluorophosphate (NOPF_6) as an oxidant. The doping state was controlled by varying the immersion time in an acetonitrilic solution of NOPF_6 . To quantify the doping level of this film, we recorded its rest potential (E_R) and electrochemically reduced (dedoped) the film by stepping the potential from E_R to $-0.4 \text{ V vs. Ag/Ag}^+$. The electric charge required for dedoping was measured using a coulometer. Variations in the electrical conductivity and Seebeck coefficient with the doping level of the chemically doped P3HT film closely matched the results obtained for the electrochemically doped film, indicating that the doping method does not markedly affect the thermoelectric properties.

Interestingly, the $\log(\text{Seebeck coefficient})-\log(\text{doping level})$ plot revealed a well-defined linear relationship. In general, the Seebeck coefficient (S) and charge density (n) of inorganic thermoelectric materials exhibit the following relationship:

$$S = \frac{8\pi^2 k_B^2}{3eh^2} m^* T \left(\frac{\pi}{3n} \right)^{\frac{2}{3}} \tag{6}$$

where k_B , e , h , m^* , and T are the Boltzmann constant, elementary charge, Planck constant, effective mass of the charge, and absolute temperature, respectively. The logarithmic transformation of both sides of Equation 6 yields a linear dependence of $\log S$ on $\log n$ with a slope of $-2/3$ (≈ -0.67). However, the slope derived from the linear relationship shown in Figure 10 (-1.08) was distinct from that of inorganic thermoelectric materials. Xuan et al. (2010) doped P3HT with NOPF_6 and analyzed the correlation between the doping level and thermoelectric properties. This correlation was different from that observed in our work (Figure 10). In our analysis, the electrical conductivity linearly increased at low doping levels and saturated at $\sim 20\%$, while the Seebeck coefficient presented a strong linear dependence. In contrast, Xuan et al. (2010) reported that the electrical conductivity continuously linearly increased and did not saturate even at higher doping levels, while the Seebeck coefficient exhibited an S-shaped curve. This deviation may be attributable to the different methods used to estimate the doping level. We directly estimated the amount of electric charges in the entire polymer film

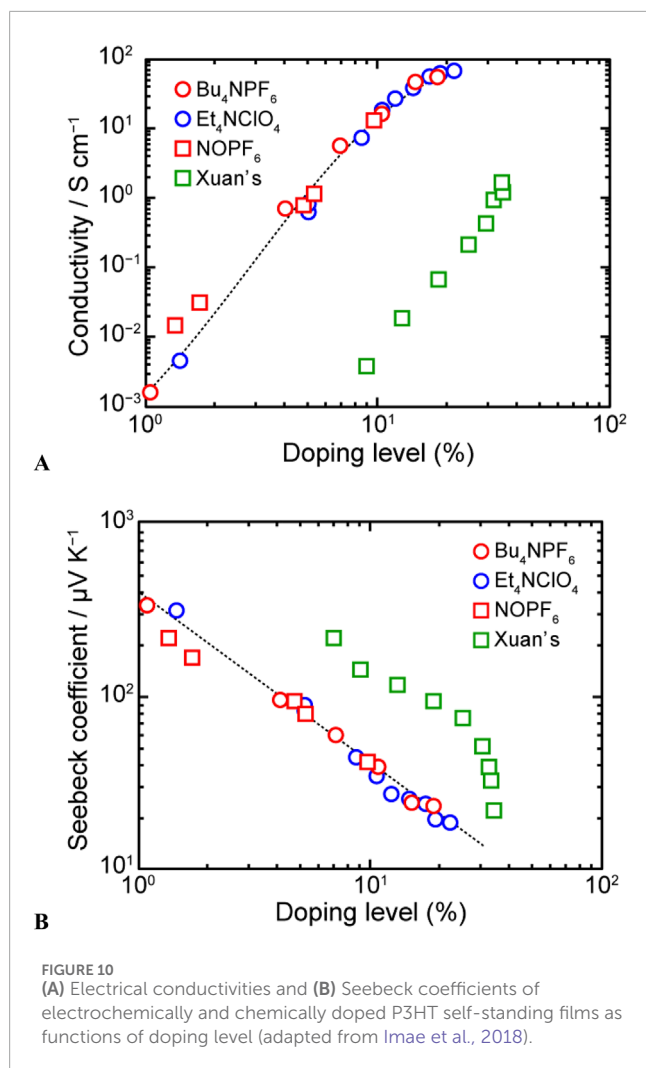


through PSC, whereas Xuan et al. (2010) calculated the doping level from the intensity ratio of the P(2p) signal derived from the dopant ion (PF_6^-) and S(2p) signal from the sulfur atom in the thiophene ring of P3HT via X-ray photoelectron spectroscopy (XPS). XPS is typically used to analyze sample surfaces, featuring an average measurement depth of ~ 10 nm. Thus, this method potentially introduces errors during the quantitation of the composition of the entire film.

To investigate the versatility of our method, we extended our investigation to other conducting polymers, including P3HT samples prepared by different methods and featuring different regioregularities (Imae et al., 2020a). The regioregularity of the P3HT samples discussed thus far was well controlled, reaching nearly 100%. However, various researchers have established distinct methods for synthesizing regioregular P3HT (Chen et al., 1995; Loewe et al., 1999; 2001; McCullough and Lowe, 1992; McCullough et al., 1993; Pouliot et al., 2016; Wang et al., 2010) through regioselective polycondensation (Figure 11A). For our study, commercially available regioregular P3HT was procured from Luminescence Technology Corp. (Lumtec) and labeled *reg*P3HT(c). We then investigated two types of P3HT without controlled regioregularity (regiorandom P3HT), which were obtained using different methods (Figures 11B, C): P3HT synthesized chemically through polycondensation without regioselectivity (*ran*P3HT(c)) and electrochemically through the electrolytic oxidative polymerization of 3-hexylthiophene (*ran*P3HT(ec)). Despite the variations in regioregularities and synthesis methods, the electrical conductivity of P3HT increased with the increasing doping level, eventually saturating, whereas the Seebeck coefficient linearly decreased (Figure 11D).

However, the maximum electrical conductivity of *ran*P3HT(c) and *ran*P3HT(ec) was only 1 S cm^{-1} , approximately two orders of magnitude lower than that of *reg*P3HT(c). The slope of the Seebeck-coefficient correlation for *ran*P3HT(c) was -1.04 , similar to that observed for *reg*P3HT(c). In contrast, the slope for *ran*P3HT(ec) was -0.63 . Chen and Inganäs (1995) reported that poly(3-octylthiophene) electrochemically synthesized by electrolytic polymerization has crosslinked structures, which affect the doping behavior, yielding results different from those observed for poly(3-octylthiophene) chemically synthesized by polycondensation. This deviation is attributable to the formation of crosslinked structures. The observed difference in the slopes of the Seebeck coefficient–doping level correlation in this study may thus be ascribed to the differences in the doping behavior of the polymer with crosslinked structures.

Next, we explored poly(3,4-ethylenedioxythiophene):poly(styrene sulfonate) (PEDOT:PSS, Figure 12A) (Imae et al., 2019), the most widely used conducting polymer in the research on thermoelectric properties (Du et al., 2022; Imae et al., 2017a; Imae, 2021; Wei et al., 2022; Xu et al., 2021). PEDOT:PSS is a polymer composite in which a π -conjugated polymer (PEDOT) is doped with a polyanion (PSS). The incorporation of PSS endows PEDOT:PSS with excellent water dispersibility, and the corresponding aqueous dispersion is commercially available on a wide scale. Generally, PEDOT is synthesized by the chemical oxidative polymerization of the corresponding monomer, EDOT. However, the resulting polymer typically contains oligomers with 6–13 EDOT units and exhibits poor film-forming properties when used alone (Elschner et al., 2011; Kirchmeyer and Reuter, 2005). Therefore, film formation is typically promoted by introducing



PSS as a dopant ion, which enables the formation of thin films with large thicknesses through spin-coating and self-standing films through drop-casting or doctor-blade coating. Additionally, when solvents with high boiling points, such as ethylene glycol (EG) or dimethyl sulfoxide (DMSO), are added in amounts of 5 wt% to the PEDOT:PSS aqueous dispersion for film formation, the electrical conductivity increases to a greater extent than that of pristine PEDOT:PSS (Ashizawa et al., 2005; Dimitrieva et al., 2009; Jönsson et al., 2003; Kim et al., 2002; Takano et al., 2012; Wei et al., 2013; 2015).

Figure 12B shows the representative cyclic voltammograms of PEDOT:PSS films, revealing that the curves of PEDOT:PSS with EG or DMSO (hereafter referred to as PEDOT:PSS-EG or PEDOT:PSS-DMSO, respectively) are shifted to the negative side in relation to that of pristine PEDOT:PSS. Thus, for these films, we calculated the doping level through PSC and correlated it with the electrical conductivity and Seebeck coefficient (Figure 12C). The electrical conductivity of PEDOT:PSS-EG or PEDOT:PSS-DMSO was more than two orders of magnitude higher than that of pristine PEDOT:PSS, irrespective of the doping level. In contrast, the Seebeck coefficient exhibited a strong linear correlation regardless of the presence of high-boiling-point solvents.

However, the corresponding slope was notably smaller than that observed for P3HT. Additionally, as the doping level increased, the plot curved downward, which was ascribed to the overoxidation of the PEDOT:PSS film. When EG or DMSO was added, the Seebeck coefficient considerably decreased compared to that of pristine PEDOT:PSS across the range of the considered oxidation levels. The slope in the linear region below an oxidation level of 10% was -0.25 .

Badre et al. (2012) and Kee et al. (2016) observed a notable increase in the electrical conductivity of spin-coated PEDOT:PSS thin films formed by adding an ionic liquid, 1-ethyl-3-methylimidazolium tetracyanoborate (EMIM:TCB, Figure 13A), highlighting the potential of these films as charge-transport materials for organic photovoltaic cells. Inspired by this finding, we attempted to create drop-cast thick films on glass substrates using an aqueous dispersion of PEDOT:PSS with EMIM:TCB and investigated their thermoelectric properties (Imae et al., 2022). Interestingly, even when the film was immersed in pure water for washing, it easily detached from the glass substrate, which resulted in the successful formation of a high-quality self-standing film (Figure 13B). In contrast, the drop-casting of PEDOT:PSS-only films led to polymer redispersion in water, which prevented the formation of self-standing films. The addition of the ionic liquid facilitated anion exchange between PSS and TCB, reducing the hydrophilicity of the polymer film and suppressing redispersion in water to promote the formation of self-standing films. Additionally, the removal of the insulating PSS through anion exchange with TCB considerably increased the electrical conductivity. The enhanced molecular arrangement of PEDOT molecules could have also contributed to the improvement of the charge-transport characteristics. Furthermore, as the amount of EMIM:TCB increased from 0 to 45 μmol , the electrical conductivity of the polymer film increased, decreasing at higher EMIM:TCB loadings (Figure 13C). The PSC results demonstrated that the charge density of the polymer film decreased upon the addition of the ionic liquid. In general, in the highly doped state, charge carriers are bipolarons exhibiting metallic conduction, whereas in low-doped states, they are polarons displaying hopping conduction. Considering that bipolarons are typically more mobile than polarons, the charge density and number of the highly mobile bipolarons decrease upon the dedoping of the polymer film. This leads to an increased proportion of the less mobile polarons and, hence, reduced charge mobility and conductivity. Thus, the electrical conductivity changes upon EMIM:TCB loading can be attributed to a trade-off between the mobility increase due to the removal of the insulating PSS and alignment of PEDOT molecules and the mobility decrease due to dedoping (Figure 13B).

To enhance the performance of organic thermoelectric materials, we developed composites of single-walled carbon nanotubes (SWCNTs) and PEDOT:PSS (Zhang et al., 2017). These composites exhibited higher electrical conductivities than individual films because of the reduction in the contact resistance between SWCNT bundles due to the preferential distribution of the electrically conductive PEDOT:PSS at the bundle junctions. Consequently, the power factor of these composites reached $300 \text{ mW m}^{-1} \text{ K}^{-2}$, representing the highest performance among organic thermoelectric materials. Additionally, by estimating

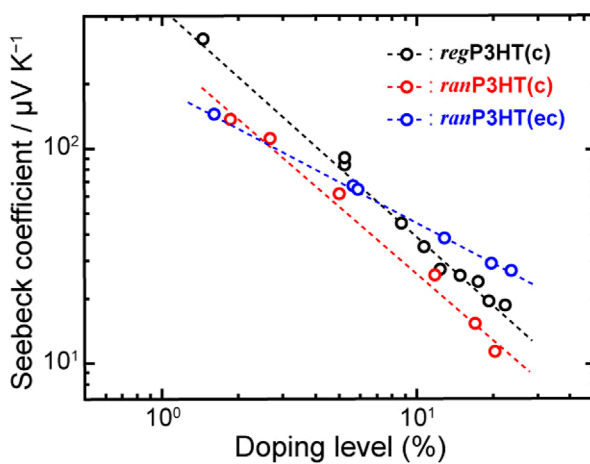
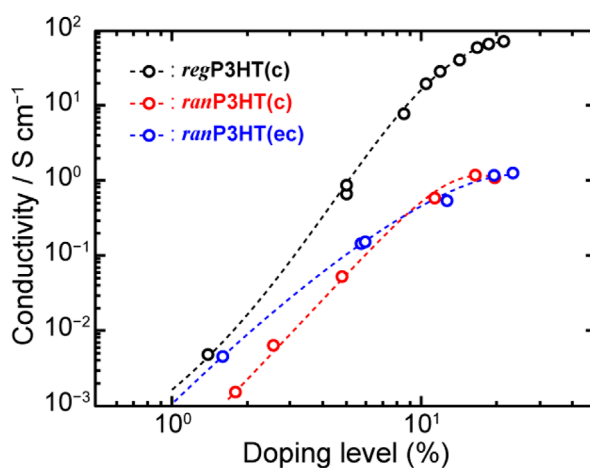
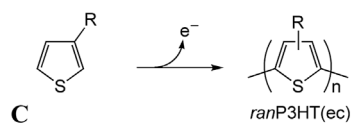
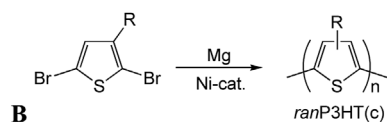
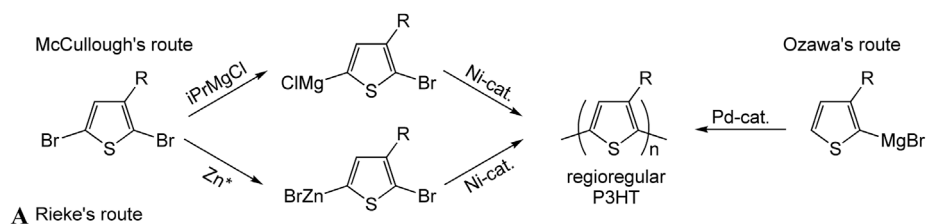
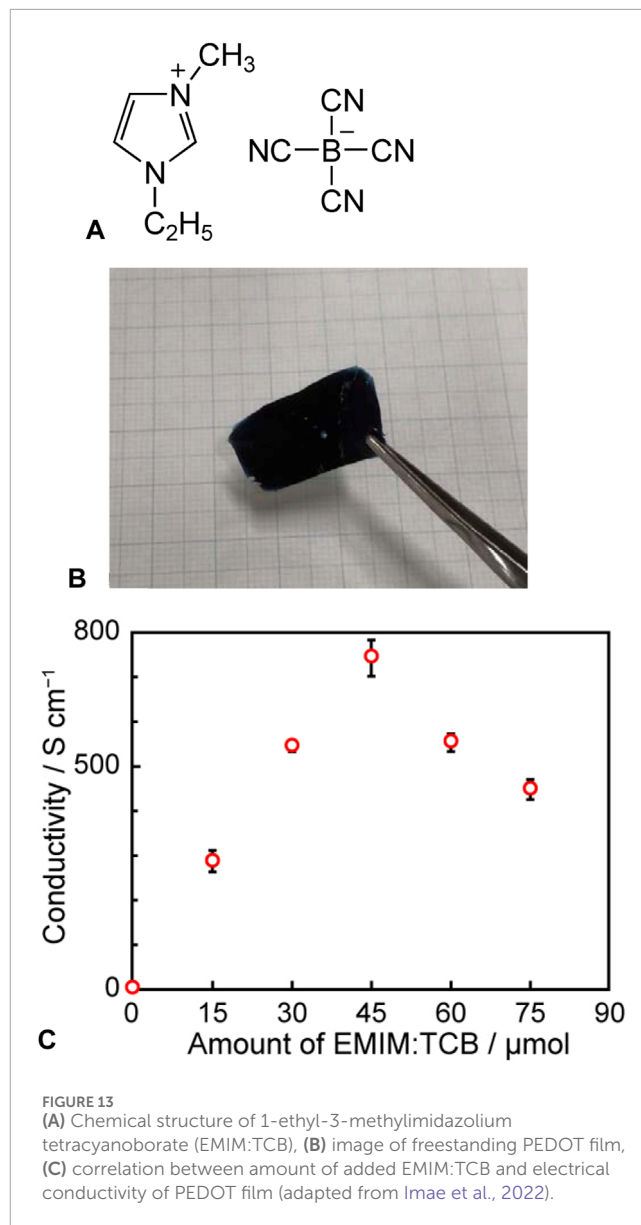
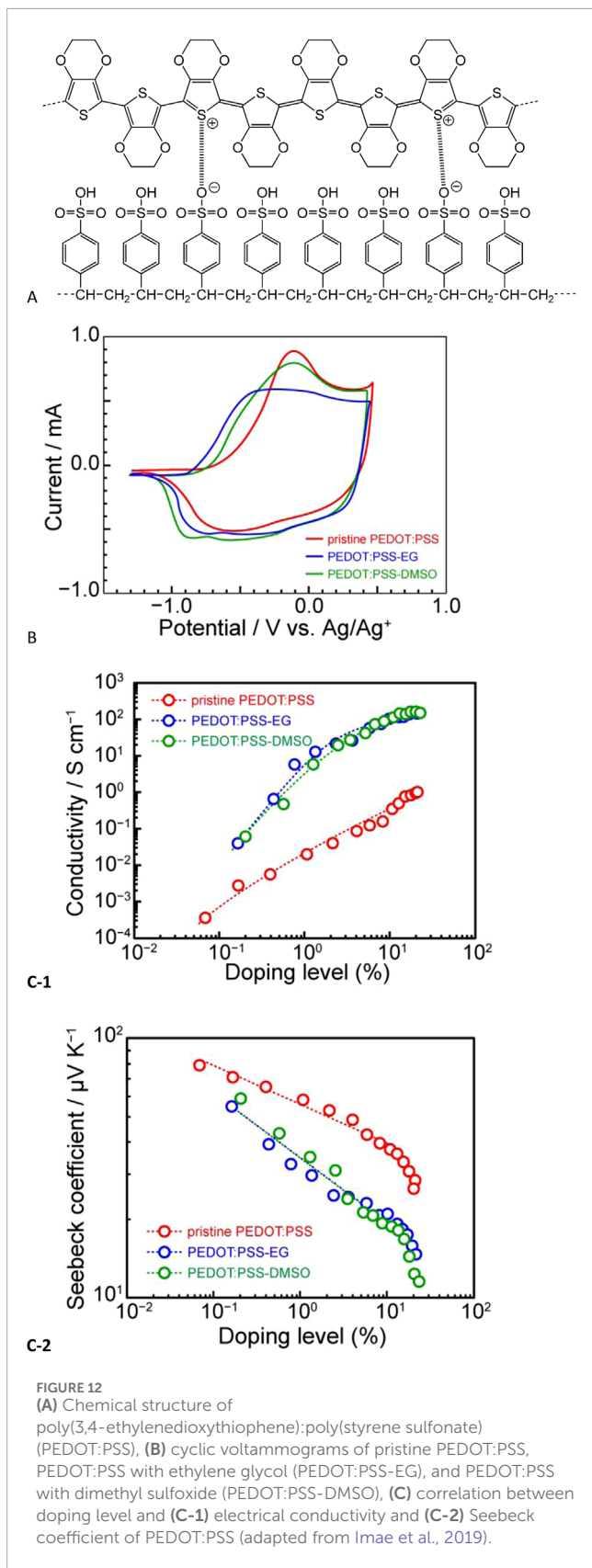


FIGURE 11 (A) Regioselective polycondensation performed to obtain regioregular P3HT (*reg*P3HT(c)), (B) syntheses of P3HT through nonregioselective polycondensation (*ran*P3HT(c)), (C) electrolytic oxidative polymerization of 3-hexylthiophene (*ran*P3HT(ec)), (D) effect of regioregularity and synthesis method on thermoelectric properties of P3HT: (D-1) electrical conductivity and (D-2) Seebeck coefficient (adapted from Imae et al., 2020a).



the thermal conductivity of the composites from reported values (Moriarty et al., 2013), we calculated ZT as ~ 0.13 at room temperature. The developed composite film can be easily produced by mixing commercially available aqueous dispersions of SWCNTs and PEDOT:PSS and offers advantages in terms of performance and the manufacturing process. To optimize the thermoelectric properties, we controlled the doping state of the composite film through PSC and quantified the charge density (Imae et al., 2021; Imae et al., 2024; Song et al., 2024). The results revealed unique behaviors reflecting the van Hove singularity (Yanagi et al., 2014) of SWCNTs, and the ongoing analysis of these findings is expected to provide deeper insights through broad charge-density control.

5 Conclusion

An electrochemical method, namely, potential-step chronocoulometry (PSC), was used to determine the charge density of conducting polymer films. This method measures the electric charge flowing between the electrode and polymer film during electrochemical doping or dedoping, allowing for the direct calculation of the number of positive charges introduced into or removed from the polymer film. Using this method, we successfully analyzed the charge-transport and thermoelectric properties of polymer films in relation to charge density. However, several challenges remain. PSC measurements can currently only be performed in wet conditions, and the quantitative accuracy of electrochemical measurements requires further refinement. Additionally, the applicability of PSC to a wider range of conducting polymers has not yet been fully explored, and distinguishing between different charge carriers, such as polarons and bipolaron species, remains a limitation. In the future, overcoming these challenges could lead to more precise correlations between charge transport and thermoelectric properties, enabling the development of advanced materials with superior thermoelectric performance. By extending the application of PSC to a broader range of materials, including nanocarbon-based composites, further insights into the design of efficient thermoelectric devices can be gained. In this regard, PSC proves to be a highly valuable analytical technique with great potential for advancing thermoelectric research.

Author contributions

II: Conceptualization, Data curation, Formal Analysis, Investigation, Methodology, Project administration, Resources,

References

- Akamatsu, H., and Inokuchi, H. (1950). On the electrical conductivity of violanthrone, iso-violanthrone, and pyranthrene. *J. Chem. Phys.* 18, 810–811. doi:10.1063/1.1747780
- Ashizawa, S., Horikawa, R., and Okuzaki, H. (2005). Effects of solvent on carrier transport in poly(3,4-ethylenedioxythiophene)/poly(4-styrenesulfonate). *Synth. Met.* 153, 5–8. doi:10.1016/j.synthmet.2005.07.214
- Badre, C., Marquant, L., Alsayed, A. M., and Hough, L. A. (2012). Highly conductive poly(3,4-ethylenedioxythiophene):poly(styrenesulfonate) films using 1-ethyl-3-methylimidazolium tetracyanoborate ionic liquid. *Adv. Funct. Mater.* 22, 2723–2727. doi:10.1002/adfm.201200225
- Bayliss, N. S. (1948). A “Metallic” model for the spectra of conjugated polyenes. *J. Chem. Phys.* 16, 287–292. doi:10.1063/1.1746869
- Bose, C. S. C., Basak, S., and Rajeshwar, K. (1992). Electrochemistry of poly(pyrrole chloride) films: a study of polymerization efficiency, ion transport during redox and doping level assay by electrochemical quartz crystal microgravimetry, pH and ion-selective electrode measurements. *J. Phys. Chem.* 96, 9899–9906. doi:10.1021/j100203a059
- Boston, R., Schmidt, W. L., Lewin, G. D., Iyasara, A. C., Lu, Z., Zhang, H., et al. (2017). Protocols for the fabrication, characterization, and optimization of n-type thermoelectric ceramic oxides. *Chem. Mater.* 29, 265–280. doi:10.1021/acs.chemmater.6b03600
- Chen, T. A., Wu, X., and Rieke, R. D. (1995). Regiocontrolled synthesis of poly(3-alkylthiophenes) mediated by Rieke zinc: their characterization and solid-state properties. *J. Am. Chem. Soc.* 117, 233–244. doi:10.1021/ja00106a027
- Chen, X., and Inganäs, O. (1995). Doping-induced volume changes in poly(3-octylthiophene) solids and gels. *Synth. Met.* 74, 159–164. doi:10.1016/0379-6779(95)03355-6
- Coughlan, C., Ibáñez, M., Dobrozhan, O., Singh, A., Cabot, A., and Ryan, K. M. (2017). Compound copper chalcogenide nanocrystals. *Chem. Rev.* 117, 5865–6109. doi:10.1021/acs.chemrev.6b00376
- Dimitrieva, O. P., Grinko, D. A., Noskov, Y., Ogurtsov, N. A., and Pud, A. A. (2009). PEDOT: PSS films—effect of organic solvent additives and annealing on the film conductivity. *Synth. Met.* 159, 2237–2239. doi:10.1016/j.synthmet.2009.08.022
- Döbbelin, M., Marcilla, R., Salsamendi, M., Pozo-Gonzalo, C., Carrasco, P. M., Pomposo, J. A., et al. (2007). Influence of ionic liquids on the electrical conductivity and morphology of PEDOT:PSS films. *Chem. Mater.* 19, 2147–2149. doi:10.1021/cm070398z
- Du, C., Cao, M., Li, G., Hu, Y., Zhang, Y., Liang, L., et al. (2022). Toward precision recognition of complex hand motions: wearable thermoelectrics by synergistic 2D nanostructure confinement and controlled reduction. *Adv. Funct. Mater.* 32, 2206083. doi:10.1002/adfm.202206083
- Elschner, A., Kirchmeyer, S., Lövenich, W., Merker, U., and Reuter, K. (2011). *PEDOT: principles and applications of an intrinsically conductive polymer*. Boca Raton: CRC Press.
- Fäid, K., and Leclerc, M. (1994). *In situ* conductivity and spectroelectrochemistry of asymmetrically disubstituted polybithiophenes: a multistep behavior. *Chem. Mater.* 6, 107–109. doi:10.1021/cm00038a003
- Ferraris, J., Cowan, D. O., Walatka, V., Jr., and Perlstein, J. H. (1973). Electron transfer in a new highly conducting donor-acceptor complex. *J. Am. Chem. Soc.* 95, 948–949. doi:10.1021/ja00784a066
- Françioso, L., and De Pascali, C. (2017). “Thermoelectric energy harvesting for powering wearable electronics,” in *Thermoelectric energy conversion: basic concepts and device applications*. Editors D. D. Pineda, and A. Reznia (Weinheim, Germany: Wiley VCH), 205–232.

Supervision, Validation, Visualization, Writing—original draft, Writing—review and editing.

Funding

The author(s) declare that no financial support was received for the research, authorship, and/or publication of this article.

Acknowledgments

We would like to thank Editage (www.editage.jp) for English language editing.

Conflict of interest

The author declares that the research was conducted in the absence of any commercial or financial relationships that could be construed as a potential conflict of interest.

Publisher’s note

All claims expressed in this article are solely those of the authors and do not necessarily represent those of their affiliated organizations, or those of the publisher, the editors and the reviewers. Any product that may be evaluated in this article, or claim that may be made by its manufacturer, is not guaranteed or endorsed by the publisher.

- Garnier, F., Horowitz, G., Fichou, D., and Yassar, A. (1996). Molecular order in organic-based field-effect transistors. *Synth. Met.* 81, 163–171. doi:10.1016/S0379-6779(96)03761-7
- Gayner, C., and Kar, K. K. (2016). Recent advances in thermoelectric materials. *Prog. Mater. Sci.* 83, 330–382. doi:10.1016/j.pmatsci.2016.07.002
- Hajlaoui, M. E., Garnier, F., Hassine, L., Kouki, F., and Bouchriha, H. (2002). Growth conditions effects on morphology and transport properties of an oligothiophene semiconductor. *Synth. Met.* 129, 215–220. doi:10.1016/S0379-6779(02)00040-1
- Hajlaoui, R., Fichou, D., Horowitz, G., Nessakh, B., Constant, M., and Garnier, F. (1997). Organic transistors using α -octithiophene and α , ω -dihexyl- α -octithiophene: influence of oligomer length versus molecular ordering on mobility. *Adv. Mater.* 9, 557–561. doi:10.1002/adma.19970090708
- Hajlaoui, R., Horowitz, G., Garnier, F., Arce-Bouchet, A., Laigre, L., El Kassmi, A. E., et al. (2004). Improved field-effect mobility in short oligothiophenes: quaterthiophene and quinquethiophene. *Adv. Mater.* 9, 389–391. doi:10.1002/adma.19970090504
- Harima, Y., Eguchi, T., and Yamashita, K. (1998). Enhancement of carrier mobilities in poly(3-methylthiophene) by an electrochemical doping. *Synth. Met.* 95, 69–74. doi:10.1016/S0379-6779(98)00035-6
- Harima, Y., Eguchi, T., Yamashita, K., Kojima, K., and Shiotani, M. (1999). An *in situ* ESR study on poly(3-methylthiophene): charge transport due to polarons and bipolarons before the evolution of metallic conduction. *Synth. Met.* 105, 121–128. doi:10.1016/S0379-6779(99)00059-4
- Harima, Y., Kunugi, Y., Yamashita, K., and Shiotani, M. (2000). Determination of mobilities of charge carriers in electrochemically anion-doped polythiophene film. *Chem. Phys. Lett.* 317, 310–314. doi:10.1016/S0009-2614(99)01378-0
- Heinze, J., Frontana-Urbe, B. A., and Ludwigs, S. (2010). Electrochemistry of conducting polymers—persistent models and new concepts. *Chem. Rev.* 110, 4724–4771. doi:10.1021/cr900226k
- Hohnholz, D., Okuzaki, H., and MacDiarmid, A. G. (2005). Plastic electronic devices through line patterning of conducting polymers. *Adv. Funct. Mater.* 15, 51–56. doi:10.1002/adfm.200400241
- Horowitz, G., Garnier, F., Yassar, A., Hajlaoui, R., and Kouki, F. (1996). Field-effect transistor made with a sexithiophene single crystal. *Adv. Mater.* 8, 52–54. doi:10.1002/adma.19960080109
- Imae, I. (2021). Reduction of graphene oxide using an environmentally friendly method and its application to energy-related materials. *Coatings* 11, 297. doi:10.3390/coatings11030297
- Imae, I., Akazawa, R., and Harima, Y. (2018). Seebeck coefficients of regioregular poly(3-hexylthiophene) correlated with doping levels. *Phys. Chem. Chem. Phys.* 20, 738–741. doi:10.1039/C7CP01114K
- Imae, I., Akazawa, R., Ooyama, Y., and Harima, Y. (2020a). Investigation of organic thermoelectric materials using potential-step chronocoulometry: effect of polymerization methods on thermoelectric properties of poly(3-hexylthiophene). *J. Polym. Sci.* 58, 3004–3008. doi:10.1002/pol.20200506
- Imae, I., Akiyama, Y., and Harima, Y. (2020b). Synthesis and properties of alkoxy-substituted oligothiophene derivatives. *J. Photopolym. Sci. Technol.* 33, 373–380. doi:10.2494/photopolymer.33.373
- Imae, I., Fujimoto, D., Zhang, L., and Harima, Y. (2017a). Electrosynthesis of a multilayer film stacked alternately by poly(3,4-ethylenedioxythiophene) and reduced graphene oxide from aqueous solution. *Electrochem. Commun.* 81, 65–69. doi:10.1016/j.elecom.2017.06.005
- Imae, I., Imabayashi, S., Komaguchi, K., Tan, Z., Ooyama, Y., and Harima, Y. (2013). Synthesis and electrical properties of novel oligothiophenes partially containing 3,4-ethylenedioxythiophenes. *RSC Adv.* 4, 2501–2508. doi:10.1039/C3RA44129F
- Imae, I., Mashima, T., Sagawa, H., Komaguchi, K., Ooyama, Y., and Harima, Y. (2015a). *In situ* conductivity measurements of polythiophene partially containing 3,4-ethylenedioxythiophene and 3-hexylthiophene. *J. Solid State Electrochem.* 19, 71–76. doi:10.1007/s10008-014-2579-8
- Imae, I., Moriwaki, K., Nawa, K., Noma, N., and Shirota, Y. (1995). Synthesis and electrical properties of novel electrochemically-doped vinyl polymers containing “end-capped” quaterthiophene and quinquethiophene as pendant groups. *Synth. Met.* 69, 285–286. doi:10.1016/0379-6779(94)02451-4
- Imae, I., Nakamura, Y., Komaguchi, K., Ooyama, Y., Ohshita, J., and Harima, Y. (2012a). Development of a simple method for fabrication of transparent conductive films with high mechanical strength. *Sci. Technol. Adv. Mater.* 13, 045005. doi:10.1088/1468-6996/13/4/045005
- Imae, I., Nawa, K., Ohseido, Y., Noma, N., and Shirota, Y. (1997a). Synthesis of a novel family of electrochemically-doped vinyl polymers containing pendant oligothiophenes and their electrical and electrochromic properties. *Macromolecules* 30, 380–386. doi:10.1021/ma961250w
- Imae, I., Noma, N., and Shirota, Y. (1997b). Electrochromic properties of a vinyl polymer containing pendant 1,4-di(2-thienyl)benzene. *Synth. Met.* 85, 1385–1386. doi:10.1016/S0379-6779(97)80284-6
- Imae, I., Ogino, R., Tsuboi, Y., Goto, T., Komaguchi, K., and Harima, Y. (2015b). Synthesis of EDOT-containing polythiophenes and their properties in relation to the composition ratio of EDOT. *RSC Adv.* 5, 84694–84702. doi:10.1039/C5RA17235G
- Imae, I., Oonishi, T., Isaak, I. S., Yamamoto, S., and Harima, Y. (2017b). Facile fabrication of transparent conductive graphene/silica composite films with high mechanical strength. *Synth. Met.* 224, 33–35. doi:10.1016/j.synthmet.2016.12.020
- Imae, I., Shi, M., Ooyama, Y., and Harima, Y. (2019). Seebeck coefficients of poly(3,4-ethylenedioxythiophene):poly(styrene sulfonate) correlated with oxidation levels. *J. Phys. Chem. C* 123, 4002–4006. doi:10.1021/acs.jpcc.8b10956
- Imae, I., Takayama, S., Tokita, D., Ooyama, Y., Komaguchi, K., Ohshita, J., et al. (2009). Development of anchored oligothiophenes on substrates for the application to the tunable transparent conductive films. *Polymer* 50, 6198–6201. doi:10.1016/j.polymer.2009.10.058
- Imae, I., Tokita, D., Ooyama, Y., Komaguchi, K., Ohshita, J., and Harima, Y. (2011). Charge transport properties of polymer films comprising oligothiophene in silsesquioxane network. *Polym. Chem.* 2, 868–872. doi:10.1039/C0PY00387E
- Imae, I., Tokita, D., Ooyama, Y., Komaguchi, K., Ohshita, J., and Harima, Y. (2012b). Oligothiophenes incorporated in a polysilsesquioxane network: application to tunable transparent conductive films. *J. Mater. Chem.* 22, 16407–16415. doi:10.1039/C2JM32259E
- Imae, I., Uehara, H., Imato, K., and Ooyama, Y. (2022). Thermoelectric properties of conductive freestanding films prepared from PEDOT:PSS aqueous dispersion and ionic liquids. *ACS Appl. Mater. Interfaces* 14, 57064–57069. doi:10.1021/acsami.2c16903
- Imae, I., Wakita, T., Imato, K., Ooyama, Y., Sakurai, Y., Asami, T., et al. (2024). Electrosynthesis and thermoelectric properties of conductive polymers with polyhedral oligomeric silsesquioxane (POSS) composites. *Energy Mater. Adv.* 5, 0119. doi:10.34133/energymatadv.0119
- Imae, I., Yamane, H., Imato, K., and Ooyama, Y. (2021). Thermoelectric properties of PEDOT:PSS/SWCNT composite films with controlled carrier density. *Compos. Commun.* 27, 100897. doi:10.1016/j.coco.2021.100897
- Ito, T., Shirakawa, H., and Ikeda, S. (1974). Simultaneous polymerization and formation of polyacetylene film on the surface of concentrated soluble Ziegler-type catalyst solution. *J. Polym. Sci. Polym. Chem. Ed.* 12, 11–20. doi:10.1002/pol.1974.170120102
- Jönsson, S. K. M., Birgersson, J., Crispin, X., Greczynski, G., Osikowicz, W., Denier van der Gon, A. W. D., et al. (2003). The effects of solvents on the morphology and sheet resistance in poly(3,4-ethylenedioxythiophene)-polystyrenesulfonic acid (PEDOT-PSS) films. *Synth. Met.* 139, 1–10. doi:10.1016/S0379-6779(02)01259-6
- Kanatzidis's group website (2024). The best thermoelectric materials. Available online at: <https://chemgroups.northwestern.edu/kanatzidis/greatthermo.html> (Accessed January 13, 2024).
- Katz, H. E., and Poehler, T. O. (2016). Innovative thermoelectric materials: polymer, nanostructure and composite thermoelectrics. *World Sci.* doi:10.1142/p980
- Kee, S., Kim, N., Kim, B. S., Park, S., Jang, Y. H., Lee, S. H., et al. (2016). Controlling molecular ordering in aqueous conducting polymers using ionic liquids. *Adv. Mater.* 28, 8625–8631. doi:10.1002/adma.201505473
- Kim, J. Y., Jung, J. H., Lee, D. E., and Joo, J. (2002). Enhancement of electrical conductivity of poly(3,4-ethylenedioxythiophene)/poly(4-styrenesulfonate) by a change of solvents. *Synth. Met.* 126, 311–316. doi:10.1016/S0379-6779(01)00576-8
- Kirchmeyer, S., and Reuter, K. (2005). Scientific importance, properties and growing applications of poly(3,4-ethylenedioxythiophene). *J. Mater. Chem.* 15, 2077. doi:10.1039/B417803N
- Kishore, R. A., Marin, A., Wu, C., Kumar, A., and Priya, S. (2019). “Thermoelectric energy harvesting,” in *Energy harvesting: materials, physics, and system design with practical examples* (Lancaster, PA: DEStech Publications Inc.), 129–166.
- Kittel, C. (2018). *Introduction to solid state physics*. global edition. 9th ed. New York: John Wiley & Sons Inc.
- Koumoto, K., and Mori, T. (2013). *Thermoelectric nanomaterials: materials design and applications*. Heidelberg: Springer.
- Kroon, R., Mengistie, D. A., Kiefer, D., Hynynen, J., Ryan, J. D., Yu, L., et al. (2016). Thermoelectric plastics: from design to synthesis, processing and structure–property relationships. *Chem. Soc. Rev.* 45, 6147–6164. doi:10.1039/C6CS00149A
- Kunugi, Y., Harima, Y., Yamashita, K., Ohta, N., and Ito, S. (2000). Charge transport in a regioregular poly(3-octylthiophene) film. *J. Mater. Chem.* 10, 2673–2677. doi:10.1039/B004434M
- Lankinen, E., Sundholm, G., Talonen, P., Laitinen, T., and Saario, T. (1998). Characterization of a poly(3-methyl thiophene) film by an *in-situ* dc resistance measurement technique and *in-situ* FTIR spectroelectrochemistry. *J. Electroanal. Chem.* 447, 135–145. doi:10.1016/S0022-0728(98)00012-6
- Lee, H. S. (2017). *Thermoelectrics: design and materials*. Chichester, UK: John Wiley & Sons, 120–163. doi:10.1002/9781118848944
- Lei, T., Pochorovski, I., and Bao, Z. (2017). Separation of semiconducting carbon nanotubes for flexible and stretchable electronics using polymer removable method. *Acc. Chem. Res.* 50, 1096–1104. doi:10.1021/acs.accounts.7b00062

- Li, J.-T., and Lei, T. (2021). Recent progress on addressing the key challenges in organic thermoelectrics. *Chem. — An Asian J.* 16, 1508–1518. doi:10.1002/asia.202100285
- Li, X., Zou, R., Liu, Z., Mata, J., Storer, B., Chen, Y., et al. (2022). Deciphering the superior thermoelectric property of post-treatment-free PEDOT:PSS/IL hybrid by X-ray and neutron scattering characterization. *npj Flex. Electron.* 6, 6. doi:10.1038/s41528-022-00138-y
- Liu, C., Xu, J., Lu, B., Yue, R., and Kong, F. (2012). Simultaneous increases in electrical conductivity and Seebeck coefficient of PEDOT:PSS films by adding ionic liquids into a polymer solution. *J. Electron. Mater.* 41, 639–645. doi:10.1007/s11664-012-1942-8
- Loewe, R. S., Ewbank, P. C., Liu, J., Zhai, L., and McCullough, R. D. (2001). Regioregular, head-to-tail coupled poly(3-alkylthiophenes) made easy by the GRIM method: investigation of the reaction and the origin of regioselectivity. *Macromolecules* 34, 4324–4333. doi:10.1021/ma001677+
- Loewe, R. S., Khersonsky, S. M., and McCullough, R. D. (1999). A simple method to prepare head-to-tail coupled, regioregular poly(3-alkylthiophenes) using Grignard metathesis. *Adv. Mater.* 11, 250–253. doi:10.1002/(SICI)1521-4095(199903)11:3<250::AID-ADMA250>3.0.CO;2-J
- Masoumi, S., O'Shaughnessy, S., and Pakdel, A. (2022). Organic-based flexible thermoelectric generators: from materials to devices. *Nano Energy* 92, 106774. doi:10.1016/j.nanoen.2021.106774
- Mazaheripour, A., Majumdar, S., Hanemann-Rowlings, D., Thomas, E. M., McGuinness, C., d'Alencon, L., et al. (2018). Tailoring the Seebeck coefficient of PEDOT:PSS by controlling ion stoichiometry in ionic liquid additives. *Chem. Mater.* 30, 4816–4822. doi:10.1021/acs.chemmater.8b02114
- McCullough, R. D., and Lowe, R. D. (1992). Enhanced electrical conductivity in regioselectively synthesized poly(3-alkylthiophenes). *J. Chem. Soc. Chem. Commun.*, 70–72. doi:10.1039/C39920000070
- McCullough, R. D., Lowe, R. D., Jayaraman, M., Ewbank, P. C., and Anderson, D. L. (1993). Design, synthesis, and control of conducting polymer architectures: structurally homogeneous poly(3-alkylthiophenes). *J. Org. Chem.* 58, 904–912. doi:10.1021/jo00056a024
- Moriarty, G. P., De, S., King, P. J., Khan, U., Via, M., King, J. A., et al. (2013). Thermoelectric behavior of organic thin film nanocomposites. *J. Polym. Sci. B Polym. Phys.* 51, 119–123. doi:10.1002/polb.23186
- Morvant, M. C., and Reynolds, J. R. (1998). *In situ* conductivity studies of poly(3,4-ethylenedioxythiophene). *Synth. Met.* 92, 57–61. doi:10.1016/S0379-6779(98)80023-4
- Murakami, T., Mori, Y., and Okuzaki, H. (2011). Effect of ethylene glycol on structure and carrier transport in highly conductive poly(3,4-ethylenedioxythiophene)/poly(4-styrenesulfonate). *Trans. Mater. Res. Soc. Jpn.* 36, 165–168. doi:10.14723/tmrj.36.165
- Natta, G., Mazzanti, G., and Corradini, P. (1967). Stereospecific polymerization of acetylene. *Stereoregular Polym. Stereospecific Polym.*, 463–465. doi:10.1016/B978-1-4831-9883-5.50084-2
- Nawa, K., Imae, I., Noma, N., and Shirota, Y. (1995). Synthesis of a novel type of electrochemically doped vinyl polymer containing pendant terthiophene and its electrical and electrochromic properties. *Macromolecules* 28, 723–729. doi:10.1021/ma00107a008
- Nawa, K., Miyawaki, K., Imae, I., Noma, N., and Shirota, Y. (1993a). Polymers containing pendant oligothiophenes as a novel class of electrochromic materials. *J. Mater. Chem.* 3, 113–114. doi:10.1039/JM9930300113
- Nawa, K., Miyawaki, K., Imae, I., Noma, N., and Shirota, Y. (1993b). A novel type of semiconducting polymers: synthesis and properties of electrochemically doped polymers containing pendant oligothiophenes. *Synth. Met.* 55, 1176–1181. doi:10.1016/0379-6779(93)90220-Q
- Nicolini, T., Shinde, S., El-Attar, R., Salinas, G., Thuau, D., Abbas, M., et al. (2024). Fine-tuning the optoelectronic and redox properties of an electropolymerized thiophene derivative for highly selective OECT-based zinc detection. *Adv. Mater. Interfaces* 11, 2400127. doi:10.1002/admi.202400127
- Nobel Prize in Chemistry (2000). Nobel prize outreach AB 2024. Available online at: <https://www.nobelprize.org/prizes/chemistry/2000/summary/> (Accessed January 1, 2024).
- Ohseido, Y., Imae, I., Noma, N., and Shirota, Y. (1996). Synthesis and electrochromic properties of a methacrylate polymer containing pendant terthiophene. *Synth. Met.* 81, 157–162. doi:10.1016/S0379-6779(96)03753-8
- Ohseido, Y., Imae, I., and Shirota, Y. (1999). Synthesis and electrochromic properties of methacrylate copolymers containing pendant terthiophene and oligo(ethyleneoxide) moieties. *Synth. Met.* 102, 969–970. doi:10.1016/S0379-6779(98)01033-9
- Ohseido, Y., Imae, I., and Shirota, Y. (2000). Electrochromic properties of new methacrylate copolymers containing pendant oligothiophene and oligo(ethyleneoxide) moieties in the presence of a polymer-gel electrolyte. *Electrochim. Acta* 45, 1543–1547. doi:10.1016/S0013-4686(99)00372-2
- Ohseido, Y., Imae, I., and Shirota, Y. (2003). Synthesis and electrochromic properties of a new family of methacrylate polymers containing pendant oligothiophenes. *J. Polym. Sci. B Polym. Phys.* 41, 2471–2484. doi:10.1002/polb.10653
- Okuzaki, H., Harashina, Y., and Yan, H. (2009). Highly conductive PEDOT/PSS microfibers fabricated by wet-spinning and dip-treatment in ethylene glycol. *Eur. Polym. J.* 45, 256–261. doi:10.1016/j.eurpolymj.2008.10.027
- Peng, S., Wang, D., Lu, J., He, M., Xu, C., Li, Y., et al. (2017). A review on organic polymer-based thermoelectric materials. *J. Polym. Environ.* 25, 1208–1218. doi:10.1007/s10924-016-0895-z
- Pouliot, J.-R., Wakioka, M., Ozawa, F., Li, Y., and Leclerc, M. (2016). Structural analysis of poly(3-hexylthiophene) prepared via direct heteroarylation polymerization. *Macromol. Chem. Phys.* 217, 1493–1500. doi:10.1002/macp.201600050
- Ravichandran, J. (2017). Thermoelectric and thermal transport properties of complex oxide thin films, heterostructures and superlattices. *J. Mater. Res.* 32, 183–203. doi:10.1557/JMR.2016.419
- Russ, B., Glauddell, A., Urban, J. J., Chabiny, M. L., and Segalman, R. A. (2016). Organic thermoelectric materials for energy harvesting and temperature control. *Nat. Rev. Mater.* 1, 16050. doi:10.1038/natrevmats.2016.50
- Salinas, G., and Frontana-Urbe, B. A. (2019). Analysis of conjugated polymers conductivity by *in situ* electrochemical-conductance method. *ChemElectroChem* 6, 4105–4117. doi:10.1002/celec.201801488
- Saxena, N., Pretzl, B., Lamprecht, X., Bießmann, L., Yang, D., Li, N., et al. (2019). Ionic liquids as post-treatment agents for simultaneous improvement of Seebeck coefficient and electrical conductivity in PEDOT:PSS films. *ACS Appl. Mater. Interfaces* 11, 8060–8071. doi:10.1021/acsami.8b21709
- Schiavon, G., Sitran, S., and Zotti, G. (1989). A simple two-band electrode for *in situ* conductivity measurements of polyconjugated conducting polymers. *Synth. Met.* 32, 209–217. doi:10.1016/0379-6779(89)90843-6
- Shirakawa, H., and Ikeda, S. (1971). Infrared spectra of poly(acetylene). *Polym. J.* 2, 231–244. doi:10.1295/polymj.2.231
- Shirakawa, H., Ito, T., and Ikeda, S. (1973). Raman scattering and electronic spectra of poly(acetylene). *Polym. J.* 4, 460–462. doi:10.1295/polymj.4.460
- Shirakawa, H., Louis, E. J., MacDiarmid, A. G., Chiang, C. K., and Heeger, A. J. (1977). Synthesis of electrically conducting organic polymers: halogen derivatives of polyacetylene, (CH)_x. *J. Chem. Soc. Chem. Commun.*, 578–580. doi:10.1039/C39770000578
- Song, J. H., Jeong, J., Park, J., Park, G., Imae, I., and Kwak, J. (2024). Enhanced performance and stability of PEDOT:PSS thin-film thermoelectrics by de-doping with nitrogen-doped graphene quantum dots. *ACS Appl. Electron. Mater.* 6, 6313–6321. doi:10.1021/acsaem.4c01357
- Sugimoto, T. (2000). Demand outlook for thermoelectric power generation. *Mater. Integr.* 13, 53–56.
- Swager, T. M. (2017). 50th anniversary perspective: conducting/semiconducting conjugated polymers. A personal perspective on the past and the future. *Macromolecules* 50, 4867–4886. doi:10.1021/acs.macromol.7b00582
- Takano, T., Masunaga, H., Fujiwara, A., Okuzaki, H., and Sasaki, T. (2012). PEDOT nanocrystal in highly conductive PEDOT:PSS polymer films. *Macromolecules* 45, 3859–3865. doi:10.1021/ma300120g
- Tan, G., Zhao, L. D., and Kanatzidis, M. G. (2016). Rationally designing high-performance bulk thermoelectric materials. *Chem. Rev.* 116, 12123–12149. doi:10.1021/acs.chemrev.6b00255
- Tang, H., Zhu, L., Harima, Y., and Yamashita, K. (2000). Chronocoulometric determination of doping levels of polythiophenes: influences of overoxidation and capacitive processes. *Synth. Met.* 110, 105–113. doi:10.1016/S0379-6779(99)00269-6
- Thackeray, J. W., White, H. S., and Wrighton, M. S. (1985). Poly(3-methylthiophene)-coated electrodes: optical and electrical properties as a function of redox potential and amplification of electrical and chemical signals using poly(3-methylthiophene)-based microelectrochemical transistors. *J. Phys. Chem.* 89, 5133–5140. doi:10.1021/j100269a048
- Toshima, N. (2017). Recent progress of organic and hybrid thermoelectric materials. *Synth. Met.* 225, 3–21. doi:10.1016/j.synthmet.2016.12.017
- Toshima, N., and Kawai, T. (2017). Preface. *Synth. Met.* 225, 1–2. doi:10.1016/j.synthmet.2017.01.012
- Tsukada, S., Nakanishi, Y., Kai, H., Ishimoto, T., Okada, K., Adachi, Y., et al. (2020). NIR-shielding films based on PEDOT-PSS/polyisiloxane and polysilsesquioxane hybrid. *J. Appl. Polym. Sci.* 137, 48367. doi:10.1002/app.48367
- Wang, Q., Takita, R., Kikuzaki, Y., and Ozawa, F. (2010). Palladium-catalyzed dehydrohalogenative polycondensation of 2-bromo-3-hexylthiophene: an efficient approach to head-to-tail poly(3-hexylthiophene). *J. Am. Chem. Soc.* 132, 11420–11421. doi:10.1021/ja105767z
- Wei, Q., Mukaida, M., Kirihara, K., Naitoh, Y., and Ishida, T. (2015). Recent progress on PEDOT-based thermoelectric materials. *Materials* 8, 732–750. doi:10.3390/ma8020732
- Wei, Q., Mukaida, M., Naitoh, Y., and Ishida, T. (2013). Morphological change and mobility enhancement in PEDOT:PSS by adding co-solvents. *Adv. Mater.* 25, 2831–2836. doi:10.1002/adma.201205158

- Wei, S., Liu, L., Huang, X., Zhang, Y., Liu, F., Deng, L., et al. (2022). Flexible and foldable films of SWCNT thermoelectric composites and an s-shape thermoelectric generator with a vertical temperature gradient. *ACS Appl. Mater. Interfaces* 14, 5973–5982. doi:10.1021/acsmi.1c21363
- Xu, Y., Jia, Y., Liu, P., Jiang, Q., Hu, D., and Ma, Y. (2021). Poly(3,4-ethylenedioxythiophene) (PEDOT) as promising thermoelectric materials and devices. *Chem. Eng. J.* 404, 126552. doi:10.1016/j.cej.2020.126552
- Xuan, Y., Liu, X., Desbief, S., Leclère, P., Fahlman, M., Lazzaroni, R., et al. (2010). Thermoelectric properties of conducting polymers: the case of poly(3-hexylthiophene). *Phys. Rev. B* 82, 115454. doi:10.1103/PhysRevB.82.115454
- Yan, H., and Toshima, N. (1999). Thermoelectric properties of alternatively layered films of polyaniline and (\pm)-10-Camphorsulfonic acid-doped polyaniline. *Chem. Lett.* 28, 1217–1218. doi:10.1246/cl.1999.1217
- Yanagi, K., Kanda, S., Oshima, Y., Kitamura, Y., Kawai, H., Yamamoto, T., et al. (2014). Tuning of the thermoelectric properties of one-dimensional material networks by electric double layer techniques using ionic liquids. *Nano Lett.* 14, 6437–6442. doi:10.1021/nl502982f
- Yao, H., Fan, Z., Cheng, H., Guan, X., Wang, C., Sun, K., et al. (2018). Recent development of thermoelectric polymers and composites. *Macromol. Rapid Commun.* 39, 1700727. doi:10.1002/marc.201700727
- Yin, Y., Tudu, B., and Tiwari, A. (2017). Recent advances in oxide thermoelectric materials and modules. *Vacuum* 146, 356–374. doi:10.1016/j.vacuum.2017.04.015
- Zhang, L., Harima, Y., and Imae, I. (2017). Highly improved thermoelectric performances of PEDOT:PSS/SWCNT composites by solvent treatment. *Org. Electron.* 51, 304–307. doi:10.1016/j.orgel.2017.09.030
- Zhao, W., Ding, J., Zou, Y., Di, C., and Zhu, D. (2020). Chemical doping of organic semiconductors for thermoelectric applications. *Chem. Soc. Rev.* 49, 7210–7228. doi:10.1039/D0CS00204F
- Zhu, T., Liu, Y., Fu, C., Heremans, J. P., Snyder, J. G., and Zhao, X. (2017). Compromise and synergy in high-efficiency thermoelectric materials. *Adv. Mater.* 29, 1605884. doi:10.1002/adma.201605884
- Zotti, G. (1998). Doping-level dependence of conductivity in polypyrroles and polythiophenes. *Synth. Met.* 97, 267–272. doi:10.1016/S0379-6779(98)00144-1